8-10-2020 1:00 PM

Staphylococcus aureus small colony variants use heme and staphyloferrin B for iron acquisition

Izabela Z. Batko, *The University of Western Ontario*

Supervisor: Heinrichs, David E., *The University of Western Ontario*

A thesis submitted in partial fulfillment of the requirements for the Master of Science degree in Microbiology and Immunology

Abstract

Iron is an essential nutrient for the bacterium *Staphylococcus aureus*. Wild-type *S. aureus* utilizes various iron acquisition systems to support growth in iron deplete conditions. *S. aureus* small colony variants (SCVs) are associated with chronic infections, yet the mechanisms by which these variants acquire iron are unknown. Mutation of *hemB*, involved in heme biosynthesis, generated a stable SCV that was auxotrophic for hemin and formed small colonies on solid media. To support growth under iron deplete conditions, my data revealed that *S. aureus hemB* synthesizes the siderophore staphyloferrin B, but not staphyloferrin A, although both siderophores could be utilized by the *hemB* mutant if provided exogenously. Additionally, I demonstrated that the *hemB* mutant, in comparison to wild-type *S. aureus*, was defective for xenosiderophore utilization, including the clinically approved drug Desferal. This study yields important insight into the mechanisms by which *S. aureus* SCVs acquire iron to cause persistent infection.

Keywords: *Staphylococcus aureus*, small colony variant, SCV, *hemB*, iron acquisition, siderophores, infection

Summary for Lay Audience

Staphylococcus aureus is a serious threat to human health and can take on a small colony variant (SCV) form. *S. aureus* SCVs grow slowly and express genes differently than normal *S. aureus* because of an altered metabolism. SCVs have been linked to chronic *S. aureus* infections that are difficult to treat. To cause these infections, *S. aureus* SCVs must get iron from the host because it is an essential nutrient. *S. aureus* has evolved several ways to acquire iron in the host, such as the use of siderophores which bind iron strongly and carry it into the cell. While the iron acquisition strategies of normal *S. aureus* have been studied, it is unknown how *S. aureus* SCVs acquire iron. Here, the iron acquisition strategies of a stable *S. aureus* SCV, the *hemB* mutant, were investigated. The *S. aureus hemB* mutant was found to have a defect in the production of one of the two staphylococcal siderophores, which was related to differences in its metabolism. The *hemB* mutant used both staphylococcal siderophores, but could not use siderophores from other organisms, unlike like normal *S. aureus*. Siderophores were not important for the *S. aureus hemB* mutant in a mouse model of infection and SCVs were less infective than normal *S. aureus*. This study contributes to our understanding of how *S. aureus* SCVs acquire iron to cause lasting infections.

Acknowledgements

First and foremost, I would like to thank my supervisor Dr. David Heinrichs for giving me the opportunity to work in his lab and for his constant support. He helped foster an environment conducive to learning which helped me thrive as a young researcher. His insight, encouragement, and guidance were invaluable to this project and my personal growth.

I would like to extend a special thank you to Dr. Ron Flannagan for his mentorship and assistance throughout the course of this project. Starting in the fourth year of my undergraduate degree, he taught me important skills and techniques that enabled me to gain confidence and independence in my research. My many discussions with Ron and his vast knowledge, expertise, and suggestions were critical for steering this project in the right direction. I would like to sincerely thank Drs. Heinrichs and Flannagan for their help in performing the mouse work for this project. Thank you Dr. Jessica Sheldon for generating the *hemB*::Sp mutant, used throughout this study.

Thank you also to my advisory committee members Dr. John McCormick and Dr. Martin McGavin. Their feedback and recommendations over the duration of this project were greatly appreciated.

Lastly, I would like to extend a thank you to all the members of the Heinrichs lab, my friends, and my family for helping make these past two years so special. This accomplishment would not have been possible without their support.

Table of Contents

List of Tables

List of Figures

List of Abbreviations

A_{385}	absorbance at 385 nm
ABC	ATP-binding cassette
agr	accessory gene regulator
α-KG	α-ketoglutarate
ALA	δ-aminolevulinic acid
Amp	ampicillin
ATP	adenosine triphosphate
CA-MRSA	community-associated MRSA
CF	cystic fibrosis
CFU	colony forming unit
Cm	chloramphenicol
CoNS	coagulase-negative staphylococci
CoPS	coagulase-positive staphylococci
Dcytb	duodenal cytochrome B
˚C	degrees Celsius
DFO	deferoxamine mesylate
DMT1	divalent metal transporter 1
DNA	deoxyribonucleic acid
Efb	extracellular fibrinogen binding protein
EfeUOB	elemental ferrous uptake system
ETC	electron transport chain
FAS	ferrous ammonium sulfate
FBS	fetal bovine serum
Fe^{2+}	ferrous iron
Fe^{3+}	ferric iron
Fhu	ferric hydroxamate uptake system
Fpn	ferroportin
Fur	ferric uptake regulator
g	gram
h	hour

HA-MRSA	hospital-associated MRSA
Hb	hemoglobin
HCP-1	heme carrier protein-1
HFE	human hemostatic iron regulator protein
HH	hereditary hemochromatosis
Hp	haptoglobin
HS	horse serum
Hts	heme transport system
Hx	hemopexin
•OH	hydroxyl radical
IAA	isoamyl alcohol
IruO	iron utilization oxidoreductase
Isd	iron-regulated surface determinant
Km	kanamycin
LB	Luria-Bertani broth
LBL	lysis buffer with lysostaphin
L-Dap	L-2,3-diaminopropionate
Lfn	lactoferrin
MALDI FT-ICR IMS	matrix-assisted laser desorption/ionization Fourier transform ion cyclotron resonance imaging mass spectrometry
MIC	minimum inhibitory concentration
MSCRAMMs	microbial surface components recognizing adhesive matrix molecules
µg	microgram
µL	microlitre
µm	micrometer
mg	milligram
mL	milliliter
mM	millimolar
min	minute
M	molar
N	normal

MRSA	methicillin-resistant *S. aureus*
NADPH	nicotinamide adenine dinucleotide phosphate
nm	nanometer
nM	nanomolar
OD_{600}	optical density at 600 nm
Φ	phage
PBG	porphobilinogen
PBS	phosphate buffered saline
PCR	polymerase chain reaction
PSM	phenol soluble modulin
RNA	ribonucleic acid
ROS	reactive oxygen species
rpm	revolutions per minute
RT	room temperature
RT-PCR	reverse transcription-PCR
SA	staphyloferrin A
SB	staphyloferrin B
SCV	small colony variant
SDS	sodium dodecyl sulfate
SDS-PAGE	SDS-polyacrylamide gel electrophoresis
SigB	sigma B
Sp	spectinomycin
SrtA	sortase A
SrtB	sortase B
Sst	staphylococcal siderophore transport system
SSTI	skin and soft tissue infection
STE	sodium chloride-Tris-EDTA buffer
$\bullet O_2^-$	superoxide anion
Tc	tetracycline
TCA	tricarboxylic acid
Tfn	transferrin

TfR1	Tfn receptor 1
TfR2	Tfn receptor 2
TMS	Tris Minimal Succinate
TSA	TSB agar
TSB	Tryptic Soy broth
WT	wild-type
w/v	weight (g)/volume (mL)
v/v	volume/volume

Chapter 1

1 Introduction

1.1 *Staphylococcus aureus*

The notorious pathogen *Staphylococcus aureus* is a Gram-positive, coagulase-positive bacterium that is spherical in shape and forms grape-like clusters. *S. aureus* asymptomatically colonizes several sites of the human body, with nasal carriage being most prevalent[1,2]. Indeed, approximately 30% of the human population are intermittent nasal carriers and about 20% are persistent nasal carriers[2]. The widespread prevalence of *S. aureus* is concerning, as individuals colonized by *S. aureus* are at an increased risk of infection by the opportunistic pathogen[3–5]. Importantly, *S. aureus* is a significant cause of morbidity and mortality, which is emphasized by reports that invasive *S. aureus* infections contribute to more deaths in the United States than HIV[6]. Owing to its ability to colonize virtually every tissue of the human body, *S. aureus* causes a wide range of infections including skin and soft tissue infections (SSTIs), bacteremia, pneumonia, endocarditis, and osteomyelitis[6–8].

The ability of *S. aureus* to acquire antibiotic resistance is a major clinical concern, as it complicates treatment of *S. aureus* infection. Notably, *S. aureus* developed resistance to penicillin and methicillin within two years of introduction of each of these antibiotics in the mid-1900s[9–11]. Methicillin-resistant *S. aureus* (MRSA) spread globally and was initially considered a nosocomial pathogen, until the emergence of community-associated MRSA (CA-MRSA) strains shifted this view within the last two decades[12,13]. Unlike hospital associated MRSA (HA-MRSA) strains that opportunistically infect immunocompromised patients, the newly emerged and genetically distinct CA-MRSA strains can infect otherwise healthy individuals[12,13]. Importantly, while CA-MRSA typically manifests as SSTIs, it can also cause more severe, and even lethal, infections such as necrotizing pneumonia and necrotizing fasciitis in diverse, otherwise healthy populations[8,12,14]. The most predominant CA-MRSA strain in North America is USA300 and, therefore, USA300 is often used in laboratories that study the molecular pathogenesis of *S. aureus*[15,16]. Investigation of *S. aureus* pathogenesis is critical to help identify novel therapeutic targets that, if perturbed, could ameliorate treatment of antibiotic-resistant *S. aureus* infection.

1.2 *S. aureus* pathogenesis

The success of *S. aureus* as a pathogen is dependent on its ability to evade the host immune system and acquire or synthesize essential nutrients. For this, *S. aureus* employs an armamentarium of virulence factors (summarized in Fig. 1). Importantly, *S. aureus* coordinates the expression of its virulence factors by sensing environmental cues and a complex network of transcription regulators[17]. The details of each of these virulence factors is beyond the scope of this project but have been reviewed extensively[17–21]. Briefly, an important facet of innate immunity, the host's first line of defense against invading pathogens, are professional phagocytes such as macrophages and neutrophils. These leukocytes target and eliminate invading pathogens, using a variety of antimicrobial effectors such as lysozyme, cationic antimicrobial peptides, and reactive oxygen species (ROS)[18,22]. Phagocytosis is facilitated by opsonization of pathogens through deposition of C3b – the resulting effector of the activated classical complement pathway – on the bacterial surface or binding of IgG to antigens on the cell surface[20]. However, *S. aureus* thwarts efficient phagocytosis by expressing virulence factors that interfere with opsonization, such as extracellular fibrinogen binding protein (Efb) which binds fibrinogen and masks C3b binding, and protein A which binds IgG in the incorrect orientation for phagocytosis[23,24]. Remarkably, phagocytosed *S. aureus* survive within leukocytes[25–27], avoiding phagocyte-mediated killing by evading antimicrobial defenses[18,22]. In fact, work by the Heinrichs lab has characterized the replication of *S. aureus* within the phagolysosome of macrophages[28]. In addition to evasion of the host immune cells, *S. aureus* secretes effectors that target and kill cells, causing tissue damage and enabling dissemination throughout the host. Secreted toxins by *S. aureus* include bi-component leukocidins, α-toxin, and phenol soluble modulins (PSMs) which form pores and damage the membranes of host cells thereby evoking cell death[29–31]. Moreover, *S. aureus* utilizes microbial surface components recognizing adhesive matrix molecules (MSCRAMMs) adhesin proteins to adhere to host extracellular matrix factors, which facilitate invasion of endothelial and epithelial cells and contribute to immune evasion[20]. In summary, *S. aureus* uses a plethora of virulence factors which enables the pathogen to prevail against host immune defences and to cause infections in host tissues.

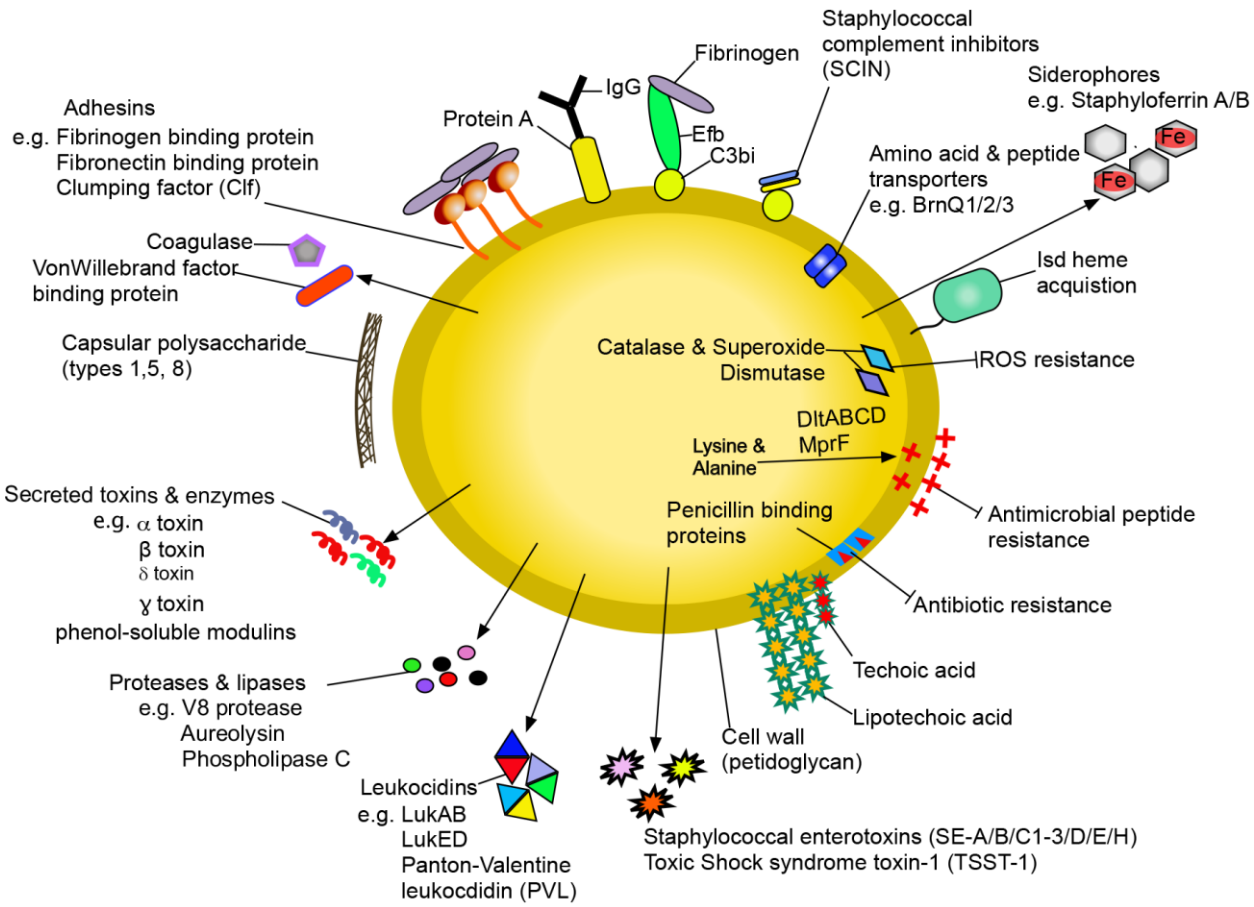

Figure 1. *S. aureus* virulence factors. Schematic of the various virulence factors employed by *S. aureus* to evade the host immune response, disseminate throughout host tissue, and acquire essential nutrients. Figure courtesy of D.E. Heinrichs.

In addition to immune evasion, *S. aureus* must acquire essential nutrients within the host, such as iron, in order to proliferate during infection. To overcome nutritional deficiencies, *S. aureus* expresses amino acid, oligopeptide, and iron transporters to import critical nutrients from the environment[32,33]. Notably, *S. aureus* is particularly adept at acquiring iron and staphylococcal iron acquisition strategies have been an ongoing research interest of the Heinrichs lab for the past two decades. This project focuses on staphylococcal iron acquisition strategies, but through a new lens – that of *S. aureus* small colony variants (SCVs), which had not been studied prior to this project. Staphylococcal iron acquisition strategies and *S. aureus* SCVs will be described in detail following background information about iron and host iron homeostasis.

1.3 Iron

1.3.1 Iron is an essential nutrient

As mentioned, iron is an essential nutrient for *S. aureus*, but it is also indispensable for almost all lifeforms, with *Borrelia burgdorferi* and *Lactobacillus* spp. among notable exceptions[34,35]. Iron is involved in many fundamental cellular processes, including DNA replication, amino acid synthesis, and cellular respiration[36]. Specifically, iron functions as a versatile catalyst because it readily alternates between the ferrous (Fe^{2+}) and ferric (Fe^{3+}) oxidation states through single electron transfers. Thus, iron participates in electron transfer and oxidation reactions and is an ideal cofactor for metalloproteins[36]. Therefore, invading pathogens such as *S. aureus* and the host both require iron to maintain cellular function and must compete for this important nutrient. Unsurprisingly, there exists an evolutionary arms race for the battle for iron with an important caveat: excess iron is toxic.

1.3.2 Iron toxicity

The same chemical properties that enable iron as a redox-active catalyst can promote the unfavourable generation of intracellular ROS through Fenton chemistry and the Haber-Weiss reaction[37,38]:

$Fe^{3+} + \bullet O_2^- \rightarrow Fe^{2+} + O_2$ (slow)

$Fe^{2+} + H_2O_2 \rightarrow Fe^{3+} + \bullet OH + OH^-$ (Fenton reaction; fast)

Net reaction:

$\bullet O_2^- + H_2O_2 \rightarrow O_2 + \bullet OH + OH^-$

ROS, such as the hydroxyl radicals generated here are powerful oxidizing agents that intoxicate cells through damage of nucleic acids, proteins, and lipids which can ultimately result in cell death unless they are neutralized[39,40]. Thus, while iron is essential for life, an excess is detrimental. In addition to ROS generated by excess iron, if too much iron is present in the blood or in tissues, it can form toxic ferric hydroxide precipitates, which are detrimental for the host[41]. These ferric hydroxide precipitates form because of the insolubility of ferric iron (Fe^{3+}) under physiological conditions – an aerobic environment with neutral pH[41,42]. Aerobic organisms must therefore maintain a delicate balance, limiting the amount of free iron through strict regulation of its acquisition and sequestration to avoid toxicity caused by ROS and ferric hydroxide precipitates.

1.3.3 Iron bioavailability is limited

Iron is one of the most abundant elements on Earth, but it is distinct from all the other nutrients required by pathogens, because it is the only nutrient not freely accessible from host tissue[42]. The insolubility of iron under physiological pH reduces the concentration of free Fe^{2+} to roughly 10^{-9} M[43]. Further limitation of the availability of iron is essential for the host to mitigate against the harmful effects of free iron. Therefore, the host strictly regulates iron metabolism and sequesters iron (outlined in the next section) to reduce the concentration of free iron to as low as 10^{-24} M[33]. Low concentrations of free iron also protect the host from invading microbes, which must acquire iron from the host environment. Approximately 10^{-6} M iron is required to support bacterial growth, which is much higher than what is freely available[33]. Thus, sequestration of free iron by the host starves invading pathogens of this essential nutrient thereby curtailing bacterial growth. This represents an important facet of the host's innate immune defense termed "nutritional immunity". More specifically, nutritional immunity is defined as the process of actively starving pathogens of essential nutrients, such as iron, to promote bacteriostasis[36,44]. However, successful pathogens have evolved mechanisms to circumvent the host's withholding strategies and still attain this essential nutrient under iron deplete conditions. Indeed, there exists an evolutionary arms race between hosts and pathogens, where invading microbes must employ a multitude of iron acquisition mechanisms to overcome host nutritional immunity to successfully colonize the host. An understanding of these iron acquisition mechanisms, such as those employed by *S. aureus*, will identify potential drug targets that, when perturbed, could limit nutrient acquisition and colonization by this invading pathogen that is difficult to treat through traditional antibiotic therapies.

1.4 Host iron homeostasis

To understand iron acquisition strategies employed by invading pathogens, such as *S. aureus*, it is important to first understand the tight regulation of iron within the host. It is essential for hosts to maintain homeotic iron concentrations within the body, as imbalances impact health and susceptibility to microbial infections[45]. Indeed, humans have several complex mechanisms to maintain incredibly low free iron levels that include regulation of iron absorption, iron storage and release from host cells, and scavenging of extracellular iron. This regulation begins in the proximal duodenum, where dietary iron absorption by enterocytes occurs, and is limited by the amount of iron stores within the body, to maintain a homeostatic level of total body iron[45,46]. Dietary iron is

either organic (heme iron) or inorganic (non-heme iron)[46–48]. The specialized transporters heme carrier protein-1 (HCP-1) and divalent metal transporter 1 (DMT1) on the surface of the enterocytes mediate the uptake of heme iron and Fe^{2+}, respectively[47,49,50]. Prior to DMT1-mediated uptake into enterocytes, Fe^{3+} is first reduced to Fe^{2+} by duodenal cytochrome B (Dcytb), a ferric reductase enzyme[47,51]. The absorbed dietary iron can either be used in cellular processes by the enterocytes, stored intracellularly, or transported out of the cell by ferroportin (Fpn)[46,47,52].

Critically, when Fe^{2+} exits cells through Fpn, it is oxidized by ceruloplasmin and Fe^{3+} is rapidly bound by transferrin (Tfn)[45,48]. Tfn is a host glycoprotein that reversibly binds Fe^{3+} with high affinity, scavenging free iron to prevent its accumulation in the blood and restricting Fe^{3+} access to invading pathogens[45]. Tfn also plays a critical role as a host iron transporter, delivering iron to target cells through Tfn receptor 1 (TfR1) or Tfn receptor 2 (TfR2) binding, triggering receptor-mediated endocytosis[45,53]. Fe^{3+} bound to Tfn is released by acidification of the endosome and is then reduced to Fe^{2+} by the ferrireductase STEAP3[45,54]. Next, DMT1 transports Fe^{2+} to the cytoplasm, where it can be utilized for cellular processes or stored intracellularly, as ferritin or hemosiderin[45,48]. The human body contains roughly 4 g of iron and the majority of it is stored within cells[45,46]. Roughly 29% of total body iron is stored as ferritin and hemosiderin[55]. Of the remaining 71%, approximately 70% is complexed to heme moieties in hemoglobin (Hb) usually contained within erythrocytes[55]. Scavenging host proteins haptoglobin (Hp) and hemopexin (Hx) rapidly bind free Hb and heme, respectively, because high levels of free heme can be toxic and stimulate growth of invading pathogens like *S. aureus* that can use heme as an iron source[33,45]. Lactoferrin (Lfn) is another host glycoprotein that, like Tfn, scavenges free Fe^{3+}, but Lfn is predominantly found in mucosal secretions[45]. Furthermore, iron metabolism is regulated systemically by the peptide hormone hepcidin[46–48]. Hepcidin is secreted by hepatocytes in response to excess iron levels and in the event of an infection as part of the immune response[46–48]. Hepcidin functions to reduce iron levels by regulating the internalization and degradation of Fpn[46–48]. Ultimately, this leads to decreased uptake of dietary iron by enterocytes and reduced iron release from host cells[46–48].

1.4.1 Diseases caused by iron homeostasis imbalance

The importance of the maintenance of host iron homeostasis is underscored by the impact on health and vulnerability to bacterial infection of iron deficiency or iron overload. For instance, anemia is

largely caused by iron deficiency, affects nearly one quarter of the global population, and is a significant cause of morbidity and mortality in young children and pregnant women[55,56]. Anemia is characterized by decreased concentration of erythrocytes, thus impaired ability to transport oxygen[56]. Furthermore, hereditary hemochromatosis (HH) is a prevalent autosomal recessive genetic disorder among individuals of Northern European descent[57,58]. HH is characterized by deregulation of iron absorption thus, increased iron levels within the body[57,58]. The majority of HH cases are associated with mutations of the human homeostatic iron regulator protein (HFE)[59]. HFE is thought to regulate the intestinal absorption of iron by regulation of hepcidin through its interaction with TfR1, but the exact mechanism of action is still unknown[59]. Iron overload caused by HH results in a multitude of clinical syndromes such as organ failure and increases host susceptibility to infectious disease due to saturation of Tfn[36,57,59]. Treatment of HH includes phlebotomy and iron chelation therapy[59]. One of the iron chelators used to treat iron overload is deferoxamine mesylate (DFO), which is particularly relevant for this study because *S. aureus* can utilize DFO as a source of iron[60–62]. DFO will be discussed in future sections, but it is important to note that treating iron overload using chelation therapy is complicated by pathogenic bacteria. However, while iron overload increases risk of infection, successful pathogens like *S. aureus* have evolved highly specialized iron acquisition mechanisms that allow for their nutritional requirements to be met, even in healthy individuals where iron homeostasis is maintained, and available iron is scarce.

1.5 *S. aureus* iron acquisition

As mentioned, to cause infection, *S. aureus* must evade the host immune system and meet its nutritional requirements. Indeed, *S. aureus* is a highly specialized pathogen and employs a vast array of virulence factors to effectively colonize virtually every tissue of the human body. Several of these virulence factors allow *S. aureus* to overcome nutritional immunity and acquire iron. The ability of *S. aureus* to meet iron nutritional requirements in a host where free extracellular iron is extremely scarce is dependent on sensing environmental signals, such as iron status, which results in expression of genes regulated by the ferric uptake regulator (Fur)[33,63].

1.5.1 Fur regulation of virulence factors

Fur mediates the *S. aureus* response to iron restricted conditions by causing a dramatic change in protein expression[64–66]. When iron is available, Fur dimerizes and binds Fur boxes, the consensus DNA sequence upstream of Fur-regulated genes and represses gene expression[33,63]. When intracellular concentrations of iron are low, iron dissociates from Fur, enabling expression of genes negatively regulated by Fur[33,63]. Interestingly, heart and kidney abscesses of *S. aureus* infected mice are likely iron restricted, as Fur-regulated genes are expressed in these niches[67,68]. Moreover, a *S. aureus fur* mutant was found to be attenuated *in vivo*, highlighting the importance of appropriate Fur regulation[65]. Studies that examined the protein profiles of *S. aureus* and an isogenic *fur* mutant identified a multitude of genes regulated by Fur[66,69]. These Fur-regulated genes included iron acquisition systems (with identified upstream Fur boxes) and virulence factors such as hemolysins that lyse erythrocytes to liberate heme iron (for which upstream Fur boxes could not be identified)[63,66,69]. Moreover, several proteins involved in metabolic processes were differentially expressed in the *fur* mutant[69]. Thus, Fur mediates a metabolic shift under iron starvation by downregulating expression of tricarboxylic acid (TCA) cycle genes and upregulating expression of glycolysis and fermentation enzymes[69]. Furthermore, Fur was found to positively regulate genes involved in biofilm formation and immunomodulation[66,70]. Therefore, Fur has a profound effect on the protein expression profile and potentiates *S. aureus* infection. This project focuses on several Fur-regulated proteins involved in the acquisition of iron.

1.5.2 Heme iron acquisition

As discussed, host iron is predominantly stored intracellularly as heme iron within erythrocytes. Interestingly, heme-iron is the preferred source of iron for *S. aureus* and it employs several virulence factors to access the heme iron pool[71]. Indeed, *S. aureus* expresses hemolysins, such as α-toxin, in response to limited iron availability to lyse heme-rich erythrocytes[66]. Lysed erythrocytes release Hb, which can be used by *S. aureus* as a source of iron[72]. Specifically, *S. aureus* uses a high-affinity heme iron acquisition system, the iron-regulated surface determinant (Isd) pathway, to capture heme-iron[72]. The Isd heme-iron uptake system is Fur-regulated and encoded by five operons: *isdA. isdB*, *isdCDEFsrtBisdG*, *isdH*, and *orfXisdI*[63,73]. The structural arrangement proposed for the Isd system resembles a funnel, which allows for heme complexed to iron to be brought in into the cell, crossing the cell wall and membrane[33]. IsdH, IsdB, and IsdA are

covalently anchored to the peptidoglycan by sortase A (SrtA) and IsdC is embedded in the cell wall by sortase B (SrtB)[72,73]. To capture heme-iron from the extracellular milieu, *S. aureus* utilizes IsdH, which binds Hp-Hb or Hb, and IsdB, which binds Hb[74,75]. Both proteins extract heme from Hb and heme is subsequently transported through the cell wall by IsdA and IsdC[76,77]. Next, IsdE and IsdF, components of an ABC transporter purportedly transfer heme across the cell membrane in an energy dependent manner[63,72,78]. Finally, IsdG and IsdI degrade internalized heme, releasing Fe^{2+} for use by *S. aureus*[67,79].

While the *S. aureus* Isd pathway for heme iron uptake has been well documented, it has been proposed that another mechanism for heme iron uptake exists[33]. Importantly, heme iron acquisition is not inhibited in Isd deletion mutants[80]. Moreover, the effect of Isd is masked by concentrations of heme that exceed 50 nM, presumably due to action of an unidentified low-affinity heme transporter[33]. It was previously speculated that the heme transport system (Hts) is involved in heme transport, as its name implies, but this theory has since been proven unlikely as Hts was found to be implicated in non-heme iron uptake[71,81,82]. Another potential heme iron transporter under investigation are the *S. aureus* proteins FepABC, which bear homology to the elemental ferrous uptake system (EfeUOB) of *Escherichia coli*[83,84]. In any case, Isd is the only *S. aureus* heme iron uptake system known to date.

1.5.3 Non-heme iron acquisition

In addition to capturing heme iron to meet its nutritional iron requirements, *S. aureus* is highly specialized to acquire non-heme iron. As mentioned, the host glycoproteins Tfn and Lfn scavenge free extracellular Fe^{3+} as a strategy to limit iron availability to invading pathogens. However, *S. aureus* utilizes siderophores to gain access to this pool of non-heme iron. Siderophores are low-molecular-weight molecules that bind Fe^{3+} with very high affinity and can effectively steal iron away from the host glycoproteins[33]. The use of siderophores to acquire free extracellular Fe^{3+} is not unique to *S. aureus*. A multitude of pathogens produce their own siderophores, each with varying affinity for Fe^{3+} [33,45]. Importantly, *S. aureus* produces two of its own siderophores, staphyloferrin A (SA) and staphyloferrin B (SB)[81,85–87]. Moreover, *S. aureus* can utilize xenosiderophores – siderophores generated by other organisms – to meet its nutritional iron requirements[61,88,89]. The non-heme iron acquisition strategies employed by *S. aureus* are summarized in Fig. 2.

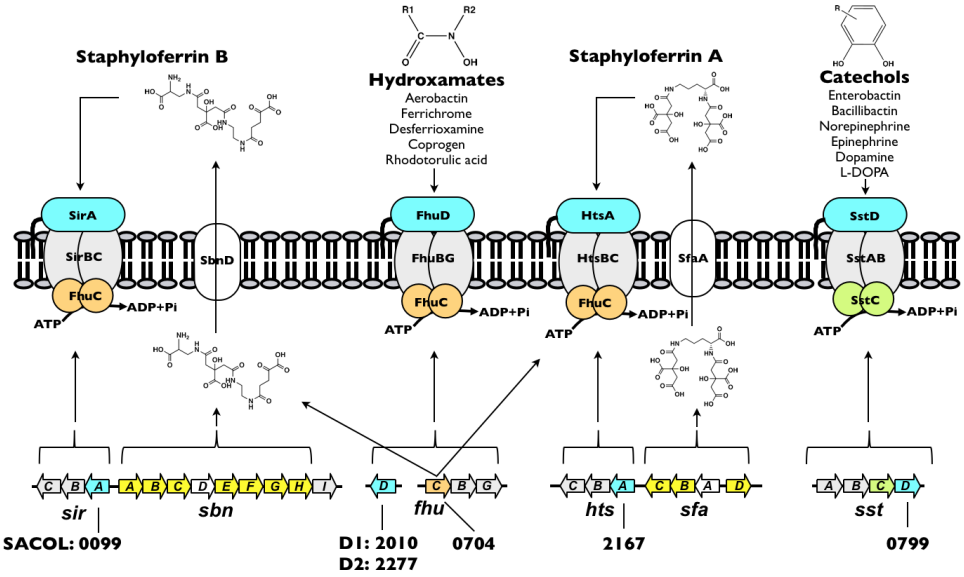

Figure 2. Non-heme iron transport in *S. aureus*. To meet nutritional iron requirements, *S. aureus* synthesizes and secretes two siderophores, SA and SB. These siderophores are taken up by the Hts and Sir transporters, respectively. *S. aureus* can also utilize hydroxamate-type and catechol-type siderophores through uptake by the Fhu and Sst transporters, respectively. Figure from Sheldon *et al.*[90].

1.5.4 Staphyloferrin A and staphyloferrin B

To acquire non-heme when intracellular iron levels are deplete, *S. aureus* produces SA and SB, two α-hydroxycarboxylate type siderophores[33]. Proteins responsible for the production and export of SA and SB are encoded in the Fur-regulated loci *sfaABCD* and *sbnABCDEFGHI*, respectively[81,85–87]. The importance of SA and SB for growth of *S. aureus* is highlighted by the significant growth defect of *in vitro* growth under iron restricted conditions when both loci are mutated[89,91,92]. However, SA and SB utilization is masked *in vivo*, as bacterial loads recovered from mice infected with *S. aureus* deficient for SA and SB utilization did not differ from those recovered from wild-type (WT) infected mice[89]. SA is comprised of two citrate units linked by a D-ornithine backbone[81,85,93]. Citrate for SA biosynthesis is solely derived from the TCA cycle citrate synthase, CitZ[92]. SfaC, a putative racemase, is believed to catalyze the formation of D-ornithine from L-ornithine, while SfaB and SfaD catalyze the assembly of the siderophore[81,85]. Following assembly, apo-SA is secreted by the efflux protein SfaA[91]. SB is chemically distinct from SA, as it is comprised of one citrate unit, one unit of α-ketoglutarate (α-KG), and two units

of L-2,3-diaminopropionate (L-Dap)[86]. Briefly, SbnA and SbnB function together, generating L-Dap and α-KG, and SbnG catalyses the formation of citrate[86,92,94,95]. Alternatively, citrate generated by CitZ can also be used for SB biosynthesis[92]. Furthermore, SbnCEFH function in the assembly of SB[86]. Therefore, the *sbn* locus encodes enzymes to generate all three SB precursor molecules and to assemble the siderophore. Export of apo-SB is mediated by the efflux protein SbnD[91]. Interestingly, SA but not SB biosynthesis is dependent on citrate derived from CitZ because SB biosynthesis can utilize citrate generated by SbnG[92]. Therefore, TCA cycle activity is critical for the generation of SA[92]. When *S. aureus* is iron starved, TCA cycle activity is decreased through Fur regulation[69]. Therefore, it stands to reason that in cells where TCA cycle activity is downregulated, for instance, in the event of nutrient deplete conditions, SB is more likely to contribute to the acquisition of non-heme iron.

Both endogenous siderophores produced by *S. aureus* function to solubilize and bind iron ferric hydroxide precipitates or to steal iron from Tfn or Lfn[33]. Ferrated SA and SB are internalized by *S. aureus* through dedicated ABC-type transporters HtsABC and SirABC, respectively[81,96]. Transcription of the SA and SB transporters occurs differentially from their associated siderophore biosynthetic genes, despite their adjacent localization[81,96]. HtsA and SirA are lipoproteins that bind Fe^{3+}-SA and Fe^{3+}-SB, respectively, in shallow, basic binding clefts[33]. The high specificity and affinity of HtsA and SirA binding pockets for their respective siderophore enables high affinity acquisition of low concentrations of extracellular SA and SB and provides a competitive advantage over other pathogens attempting to capture *S. aureus* siderophores[82,97]. Transport of Fe^{3+}-siderophore complexes across the membrane by the heterodimeric permeases HtsBC and SirBC is an energetic process powered by the genetically unlinked ATPase, FhuC[81,98].

1.5.5 Xenosiderophores

In addition to the endogenous siderophores SA and SB, *S. aureus* utilizes xenosiderophores to acquire iron within the host[61,88,89]. Importantly, *S. aureus* must compete with not only the host, but also other microorganisms for the limited quantities of available iron. Many of these microorganisms generate their own siderophores, which *S. aureus* has evolved to appropriate to meet its own nutritional requirements[61,88,89]. The appropriation of non-endogenous siderophores, such as hydroxamate and catechol-type siderophores by *S. aureus* is mediated by specialized uptake systems[61,88,89].

Specifically, *S. aureus* does not synthesize hydroxamate-type siderophores, but it can utilize them through the ferric hydroxamate uptake (Fhu) system[61,88]. The Fhu system is comprised of two integral transmembrane proteins, FhuBG, the FhuC ATPase, and two paralogous Fe^{3+}-hydroxamate binding lipoproteins, $FhuD_1$ and $FhuD_2$[61,88]. A multitude of hydroxamate-type siderophores such as ferrichrome, coprogen, and aerobactin are taken up by Fhu and promote growth of *S. aureus*[88]. Notably, desferrioxamine B is a hydroxamate-type siderophore generated by *Streptomyces pilosus* that is utilized by *S. aureus* through the Fhu transport system[62,99]. The drug DFO, which is sold by Novartis under the name Desferal and is widely used in iron chelation therapy to treat iron overload caused by HH, is the mesylate salt of desferrioxamine B[60,99]. Importantly, previous work by the Heinrichs lab has demonstrated that *S. aureus* uses DFO as a source of iron and treatment of *S. aureus* infected mice with DFO exacerbates infection, as indicated by higher bacterial burdens in the kidneys and liver and increased abscess formation relative to the control treated mice[61,88,99].

Moreover, *S. aureus* expresses the staphylococcal siderophore transport system (Sst) which allows the appropriation of catechol-type siderophores such as enterobactin and catecholamine stress hormones as sources of iron[89]. Catecholamine stress hormones, such as epinephrine and norepinephrine, reduce Fe^{3+} bound to Tfn, thereby liberating Fe^{2+} and can subsequently form complexes with the released iron[89,100]. Uptake of ferrated stress hormones and catechol-type siderophores in *S. aureus* is mediated by the SstA and SstB transmembrane proteins, SstC ATPase, and catechol binding lipoprotein, SstD[89,101]. Interestingly, the affinity of SstD for its ligands is low compared to HtsA and SirA, but this sacrifice likely allows for a greater diversity of ligands[82,89,97]. Work by the Heinrichs lab has shown that expression Sst contributes to virulence of *S. aureus* in a murine model of systemic infection[89]. Specifically, mice infected with a *S. aureus* mutant deficient for Sst, Sir and Hts had reduced bacterial burdens in the heart, liver, and kidneys relative to mice infected with the *S. aureus* mutant deficient for Sir and Hts alone[89]. Thus, it appears that the combination of each of these iron transport systems is essential for full fitness of *S. aureus in vivo*.

1.6 *S. aureus* small colony variants

S. aureus infections are difficult to treat and can persist despite administration of antibiotic therapy that should normally resolve infection[102]. Notably, *S. aureus* SCVs were first linked to persistent

infections in 1995 and have since become an important area of research[103]. An understanding of *S. aureus* SCVs is essential for the development of novel therapeutics that specifically target and eliminate persistent populations of *S. aureus*.

As their name implies, *S. aureus* SCVs form small colonies – roughly one-tenth of the size of WT *S. aureus* – when grown on solid media[104]. *S. aureus* SCVs represent a slow-growing subpopulation of *S. aureus* that have increased resistance to antibiotics and persistence within the host[102,104]. Interestingly, formation of SCVs is not unique to *S. aureus*. Indeed, *Salmonella enterica* serotype Typhi SCVs were first identified over a century ago and SCVs have been described for many other bacterial genera and species, such as *E. coli* and *Pseudomonas aeruginosa*[104–106]. Thus, SCV formation seems to be a common survival strategy employed by bacteria.

The clinical relevance of *S. aureus* SCVs is underscored by the routine isolation of SCVs from patients with persistent *S. aureus* infections[103,107]. Particularly, *S. aureus* SCVs are highly prevalent among cystic fibrosis (CF) patients with chronic recurrent lung infections and are associated with worse clinical outcomes[107,108]. Clinical isolates of *S. aureus* SCVs are unstable and have a high frequency of reversion to the normal colony phenotype[103]. *S. aureus* SCVs often arise in response to environmental stressors, such as exposure to aminoglycosides, other antimicrobials, and acidic pH[109–111]. However, the spontaneous emergence of *S. aureus* SCVs in the absence of any selective pressure has been characterized[112]. Therefore, *S. aureus* SCVs are considered a normal part of the *S. aureus* life cycle[112].

Importantly, characterization of clinically isolated *S. aureus* SCVs has determined that many SCVs arise from mutations in hemin or menadione biosynthetic genes, resulting in bacteria that are auxotrophic for these metabolites (i.e. the SCV is unable to synthesize a particular metabolite and must therefore acquire it from the environment)[104,113,114]. Indeed, provision of hemin (ferric chloride heme) or menadione was found to stimulate growth of hemin- or menadione-auxotrophs, respectively[103,104]. Interestingly, studies that examined the origin of menadione-auxotrophic SCVs isolated from patient samples identified mutations in several genes of the *men* operon, implicated in the menadione biosynthetic pathway, that can result in the formation of SCVs[115,116]. For instance, Lannergård *et al.* found three *S. aureus* SCVs that resulted from a single base pair substitution that introduced an early stop codon, from deletion of a 9 base-pair sequence, or from a frame shift mutation in *menB*[116]. Moreover, they determined that the genetic basis of SCV reversion to the normal colony phenotype was either directly by reversion to

the WT sequence, amino acid substitution, an additional mutation, or deletion of the mutated residues[116]. An earlier study by Schaff *et al.* also identified mutations associated with the spontaneous formation of SCVs when WT *S. aureus* was exposed to a sub-minimal inhibitory concentration (MIC) of the aminoglycoside gentamicin[117]. While other mutations have been linked to the formation of SCVs, such as those involved in RNA processing, my project focuses on a *S. aureus hemB* mutant[102].

The *hemB* gene encodes δ-aminolevulinic acid (ALA) dehydratase that catalyzes the synthesis of porphobilinogen (PBG) as part of the hemin biosynthetic pathway, encoded in part by the *hemAXCDBL* operon[118]. Thus, mutation of *hemB* results in deficient hemin biosynthesis and hemin auxotrophy[113]. Importantly, *S. aureus* SCVs isolated from patients are often hemin auxotrophs[103,104,114]. Moreover, it has been shown that site-directed mutagenesis of the *hemB* gene generates a stable *S. aureus* SCV[113]. The use of genetically engineered SCVs is paramount for the characterization of *S. aureus* SCVs, as clinical isolates have a high rate of reversion to the normal colony phenotype[103,107]. Indeed, various studies have made use of the *S. aureus hemB* mutant, as an archetype for the characterization of SCVs. For instance, a *S. aureus hemB* mutant was employed in a murine model of osteomyelitis to examine fitness of SCVs *in vivo*[119]. Interestingly, this study revealed that the *hemB* mutant had reduced fitness relative to WT *S. aureus*, but the SCV established an infection, as indicated by bacterial burdens recovered from infected femurs and bone destruction[119].

Notably, *S. aureus* auxotrophic for hemin manifest as SCVs due to aberrant electron transport[104]. Hemin is involved in the biosynthesis of the cytochrome component of the electron transport chain (ETC)[104]. Thus, *S. aureus hemB* mutants have a defective ETC leading to reduced membrane potential and capacity to synthesize ATP[104,113]. Importantly, this metabolic defect causes a dramatic shift in the gene expression and phenotypic changes characteristic of *S. aureus* SCVs[113,120–123]. As mentioned, *S. aureus* SCVs display slow growth and small colony size on solid media due to decreased metabolic activity[104]. *S. aureus* SCVs also have increased biofilm formation, adhesion, and are reported to persist within host cells which enables host immune evasion and protects against antimicrobials[102,124,125]. Moreover, changes in membrane potential contribute to resistance to cationic antimicrobials such as aminoglycosides, while decreased cell wall synthesis provides resistance against β-lactam antibiotics[104,123]. Furthermore, SCVs have decreased pigmentation and hemolytic activity compared to WT *S. aureus*[103,104]. The basis behind

differential virulence factor expression of SCVs is related to changes in regulation by the alternative transcription factor sigma B (SigB) and the accessory gene regulator (*agr*) system[102,126]. RNAIII is the effector molecule of the *S. aureus agr* quorum-sensing system[127]. RNAIII upregulates the expression of extracellular virulence factors, like hemolysins and proteases, and downregulates the expression of cell-wall associated proteins such as adhesins[127]. Studies have identified that virtually no RNAIII is detectable in *S. aureus* SCVs, likely due to increased RNAIII degradation by the RNA degradasome[102,123,124]. Thus, a defect in *agr* RNAIII expression may contribute to the downregulation of toxin expression in *S. aureus* SCVs, and the upregulation of adhesins. However, Vaudaux *et al.* suggested that increased adhesin expression of the *S. aureus hemB* mutant was *agr*-independent[124]. Indeed, Mitchell *et al.* postulated that elevated SigB activity in *S. aureus* SCVs has a more profound effect on the expression of virulence factors than the *agr* system, especially in biofilm formation[126]. Regardless, SigB and *agr* are interconnected and part of the complex regulatory networks that govern *S. aureus* SCV virulence factor expression[17]. In addition to altered virulence factor expression, a metabolic shift away from oxidative phosphorylation occurs in response to defective hemin biosynthesis, as enzymes involved in the TCA cycle are downregulated, and enzymes of the glycolytic and fermentation pathways are upregulated[120,128]. In summary, *S. aureus* SCVs have decreased metabolic activity and an altered gene expression profile compared to WT *S. aureus*, which results in a dramatically different phenotype.

1.7 Project rationale and hypothesis

Over the last two decades, many of the iron acquisition strategies employed by *S. aureus* have been uncovered. Remarkably, *S. aureus* is highly specialized to acquire iron and has evolved many strategies to gain access to this essential nutrient in the host, enabling infection. As mentioned, the generation of SA by *S. aureus* requires TCA cycle activity and ATP hydrolysis is required for the transport of all siderophores utilized by *S. aureus* into the cell. While the iron acquisition strategies employed by WT *S. aureus* have been well characterized, it is unknown how *S. aureus* SCVs acquire iron. *S. aureus* SCVs are linked to chronic recurrent infections that are difficult to treat because SCVs may persist intracellularly, evading the host immune system and have decreased susceptibility to therapeutic treatments. Importantly, *S. aureus* SCVs drastically differ from WT *S. aureus*, as they exhibit altered metabolic activity, morphology, and gene expression. It remains

unknown whether these factors affect the acquisition of iron by *S. aureus* SCVs, as nothing is known about *S. aureus* SCV iron acquisition mechanisms. Due to the fact that SCVs are infectious, I hypothesized that *S. aureus* SCVs must utilize one or more of the *S. aureus* iron acquisition systems to acquire iron and sustain growth.

1.8 Research objectives

To address my hypothesis, the following research objectives were pursued:

1. Characterize the *S. aureus* USA300 *hemB*::Sp mutant and define conditions for the *in vitro* study of iron acquisition strategies employed by SCVs.
2. Determine which of the iron acquisition systems active in WT *S. aureus* are important for *in vitro* growth of *S. aureus* SCVs.
3. Determine the contribution of these iron acquisition systems to *S. aureus* SCV virulence in a murine model of infection.

Chapter 2

2 Materials and Methods

2.1 Bacterial strains, plasmids and growth media

All bacterial strains and plasmids used in this study are listed in Table 1. *S. aureus* USA300 LAC cured of its endogenous antibiotic resistance plasmid served as the WT staphylococcal strain for this study. *E. coli* DH5α was used for cloning purposes and was cultured in Luria-Bertani broth (LB; Difco). *S. aureus* strains were grown in either Tryptic Soy broth (TSB; Wisent) or Tris Minimal Succinate (TMS). TMS was made as previously described[129]: 20 mL of a 25x Tris minimal salts stock (145 g of NaCl, 92.5 g of KCl, 27.5 g of NH_4Cl, 3.55 g of Na_2SO_4, 6.8 g of KH_2PO_4 dissolved in 1 L H_2O) was added to 6.05 g of Tris base, 8.3 g of sodium succinate, 5 g of casamino acids (Difco), and 450 mL H_2O, then pH was adjusted to 7.4 before autoclaving. Prior to use, 10 µL of a filter-sterilized additives mixture of 1 mL of tryptophan (10 mg/mL), 1 mL of cysteine (11 mg/mL), and 0.5 mL volumes of thiamine (16.9 mg/mL), nicotinic acid (1.23 mg/mL), pantothenic acid (0.5 mg/mL), biotin (0.01 mg/mL), $MgCl_2$ (95.3 mg/mL), and $CaCl_2$ (11.1 mg/mL) was incorporated for each millilitre of TMS. Media were prepared using water purified with a Milli-Q water filtration system (EMD Millipore, Billerica, MA). Bacterial strains were stored in 15% (v/v) glycerol at -80˚C and streaked out on solid media as needed. LB agar and TSB agar (TSA) were prepared by the addition of 1.5% (w/v) Bacto agar (Difco). The antibiotics spectinomycin (Sp; 300 µg/mL), chloramphenicol (Cm; 12 µg/mL), tetracycline (Tc; 4 µg/mL), and kanamycin (Km; 50 µg/mL) were added to media as required for *S. aureus*; ampicillin (Amp; 100 µg/mL) was added where required for *E. coli*. Bacteria were incubated at 37˚C, with constant shaking (225 rpm) where required, unless indicated otherwise.

Table 1. Bacterial strains and plasmids used in this study.

Strain or Plasmid	Description[a]	Source or Reference
E. coli		
DH5α	F- Φ_{80} dLacZΔM15 *recA1 endA1 gyrA96 thi-1 hsdR17* (r_k^-, m_k^+) *supE44 relA1 deoR* Δ(*lacZYA-argF*)U169phoA	Promega
S. aureus		
H2	RN4220 r_k^- m_k^+; accepts foreign DNA	Lab stock
H114	RN2564; (Φ80α) Ω25 [Tn551] pig-131	Lab stock
H2508	USA300 LAC; cured of antibiotic resistance plasmid	Lab stock
H627	Newman; WT clinical osteomyelitis isolate	Lab stock
H2993	USA300 *sfa*::Km	[130]
H2936	USA300 *sbn*::Tc	[130]
H2949	USA300 *sfa*::Km *sbn*::Tc	[130]
H2533	USA300 Δ*hts*	Lab stock
H803	Newman *sirA*::Km	[96]
H3044	USA300 *fhuD*$_1$::Km *fhuD*$_2$::Tc	[99]
H2935	USA300 *hemB*::Sp	This study
H3716	USA300 *hemB*::Sp *sfa*::Km	This study
H3802	USA300 *hemB*::Sp *sbn*::Tc	This study
H3717	USA300 *hemB*::Sp *sfa*::Km *sbn*::Tc	This study
H4104	USA300 *hemB*::Sp Δ*hts*	This study
H4105	USA300 *hemB*::Sp *sirA*::Km	This study
H4102	USA300 *sfa*::Km Δ*sbnG*	This study
H4103	USA300 *hemB*::Sp *sfa*::Km Δ*sbnG*	This study
Plasmids		
pALC2073	Shuttle vector; Amp^R in *E. coli*; Cm^R in *S. aureus*	[131]
p*hemB*	pALC2073 derivative for expression of *hemB*; Cm^R	This study
p*citZ*	pALC2073 derivative for expression of *citZ*; Cm^R	[92]
pKOR1Δ*sbnG*	pKOR1 derivative for in-frame, markerless deletion of *sbnG*; Cm^R	[92]

a. Km; kanamycin resistance determinant, Tc; tetracycline resistance determinant, Sp; spectinomycin resistance determinant, Amp^R; ampicillin-resistant, Cm^R; chloramphenicol-resistant.

2.2 General molecular genetic methodologies

2.2.1 *S. aureus* chromosomal DNA isolation

A single colony of *S. aureus* was picked off a TSA plate and grown overnight in TSB. Then, 500 µL of the overnight culture was pelleted, resuspended in 200 µL of sodium chloride-Tris-EDTA buffer (STE; 75 mM NaCl, 25 mM EDTA, 20 mM Tris-HCl pH 7.5), and 25 µL STE-lysostaphin (50 µg lysostaphin dissolved in 200 µL STE) was added. The sample was incubated at 37°C for at least 1 h, to allow lysis of *S. aureus* cells. Next, 20 µL of 10% (w/v) sodium dodecyl sulfate (SDS) and 20 µL Proteinase K (20 mg/mL) were added and the sample was incubated for at least 2 h at 55°C. Then, 80 µL 5M NaCl and 320 µL 25:24:1 phenol:chloroform:isoamyl alcohol (IAA) were added to the sample, which was mixed by inversion and spun at 19,000 × g 10 min before the aqueous layer was removed and added to a new 1.5 mL microcentrifuge tube. Next, 300 µL 24:1 chloroform:IAA was added, the sample was mixed by inversion, and spun at 19,000 × g for 10 min before the aqueous layer was removed and added to a new tube. To precipitate the genomic DNA, 400 µL isopropanol was added and the sample was gently mixed by inversion. DNA pellets were spun at 19,000 × g for 10 min, isopropanol was removed, and pellets were washed with 70% ethanol (stored at -20°C). DNA pellets were fully dried before resuspension in in H_2O.

2.2.2 Plasmid DNA purification

Plasmid DNA was purified using a E.Z.N.A. Plasmid Mini Kit (Omega Bio-tek) according to the manufacturer's instructions. To prepare plasmid DNA from *S. aureus*, 250 µL of Solution I-lysostaphin (50 µg lysostaphin dissolved in 1 mL Solution I) was added to each sample and samples were incubated at 37°C for a minimum of 1 h, until cells were lysed. Plasmids used are listed in Table 1.

2.2.3 Polymerase chain reaction (PCR)

PCR was performed using Taq polymerase (New England Biolabs) or Phusion polymerase (Thermo Fischer Scientific) according to manufacturer's instructions. Primers were designed using MacVector software (MacVector Inc. Apex, NC) and the published *S. aureus* USA300 FPR5737 genome[132]. Primers used in this study are summarized in Table 2. PCR products were run on 1% (w/v) agarose gels in 1 × TAE (40 mM Tris, 20 mM acetic acid, and 1 mM EDTA (pH 8.0)) with 1 kB DNA ladder (FroggaBio) to analyze amplicon size.

2.2.4 Restriction digest and ligation reactions

Restriction digests were performed using SacI and KpnI enzymes purchased from New England Biolabs according to manufacturer's instructions. Linear DNA fragments were purified directly from restriction reactions using the E.Z.N.A. Gel Extraction Kit (Omega Bio-tek) as per manufacturer's instructions. Ligation of linear DNA fragments was performed using T4 DNA ligase (New England Biolabs).

2.2.5 Colony PCR

Toothpick aliquots of patched colonies were resuspended in 50 µL of lysis buffer with lysostaphin (LBL; 50 µg lysostaphin resuspended in 1.25 mL of lysis buffer (25 mM Tris-HCl, 50 mM glucose, 150 mM NaCl, 10 mM EDTA; pH 8.0)). Samples were incubated at 37°C for 1 h before 50 µL H_2O and 2 µL of 10% (w/v) SDS were added. Samples were heated to 95°C for 10 min, then cooled at room temperature (RT) for 10 min. Next, 102 µL 25:24:1 phenol:chloroform:IAA was added and samples were incubated at RT for 30 min. Samples were centrifuged at 19,000 × g for 10 min and 10 µL was removed from the aqueous layer, which was diluted in 90 µL water. The diluted sample was used as the template for PCR.

Table 2. Oligonucleotides used in this study.

Primer pair	Sequence[a]	Application
hemB-F-SacI	TTTTTTGAGCTCTTATTTATCTAAATAGCG ACAAATGTC	Confirmation of the *hemB*::Sp mutation; complementation of the *hemB*::Sp mutant
and		
hemB-R-KpnI	TTTTTTGGTACCGATTTTAGAAAGTAGGGGC	
sfa-F-AgeI	TTTTTTACCGGTTGCAAAGCATATGTAGTA TAACTTGTCAACTTAG	Confirmation of the *sfa*::Km mutation
and		
sfa-R-AgeI	TTTTTTACCGGTGTATAGATTGTATTTAAT AAGTTAATGTAATC	
sbn-F	TAGCCTCCTTCGTGATGTAT	Confirmation of the *sbn*::Tc mutation
and		
sbnC-R	ACTGCTCTGACATCACAAAA	
or		
sbn-R	GATGCCTATCCAAATTGCTA	
hts-F	AAGCCTGTGCCGCTTCAGGT	Confirmation of the Δ*hts* mutation
and		
hts-R	ACGTTATTGCGTACGCCTGCCA	
sirA-F	AGTAGCATCGTAAAACTCCT	Confirmation of the *sirA*::Km mutation
and		
sirA-R	TAATTCATACTAAATCGTGATAATGAT	
sbnG-F	TTAAAGGCATCATCGAGGC	Confirmation of the Δ*sbnG* mutation
and		
sbnG-R	TTCACCTTGAGATGCAACTT	

a. Restriction enzyme recognition sites are underlined

2.3 Phage transduction

2.3.1 Isolation of phage (Φ80α)

A single colony of *S. aureus* RN2564 (carrying Φ80α) was picked off a TSA plate and grown overnight in TSB. The overnight culture was sub-cultured in 25 mL TSB to an optical density at 600 nm (OD_{600}) of 0.01 and grown until an OD_{600} of 0.3 was reached (~2.5 h). For induction of Φ80α, mitomycin C (2 μg/mL) was added and the culture was incubated for 3-4 h at 32ºC with slow shaking (80 rpm) until complete lysis occurred. Finally, the culture was filtered through a 0.2 μm filter and the Φ80α stock was stored at 4ºC.

2.3.2 Preparation of a transducing lysate

A single colony of the donor *S. aureus* strain carrying the desired mutation was picked off a TSA plate and grown overnight in TSB with 0.5 mM $CaCl_2$. The overnight culture was sub-cultured in 10 mL TSB with 0.5 mM $CaCl_2$ starting at an OD_{600} of 0.1 and the culture was grown at 37ºC with shaking to an OD_{600} of 0.7-1.0. Then, dilutions of Φ80α stock were prepared with phage buffer (0.1 M $MgSO_4$, 0.4 M $CaCl_2$, 2.5 M Tris pH 7.8, 5.9 g/L NaCl, 1.0 g/L gelatin) and 200 μL *S. aureus* was combined with 100 μL of phage for each of the phage dilutions. No bacteria (phage only) and no phage controls were run to ensure sterility. After a 5 min incubation at RT, the phage-bacteria mix was added to melted top agar (0.8% (w/v) TSB agar) and poured on top of TSA plates containing 4 mM $CaCl_2$ for each dilution of phage. After an overnight incubation at 37°C, phage buffer was added to the plate with the phage dilution where Φ80α almost completely cleared the lawn of bacteria. The selected plate was incubated for ~4 h on a rocker at RT, then the top agar was collected, agar was broken up by pipetting, and the mixture was centrifuged at 3,000 × g for 15 min. Finally, the supernatant was filter sterilized twice, first with a 0.45 μm filter followed by a 0.2 μm filter and the donor phage lysate was stored at 4ºC.

2.3.3 *S. aureus* phage transduction

A single colony of the recipient *S. aureus* strain was picked off a TSA plate and grown overnight in TSB with 0.5 mM $CaCl_2$. The overnight culture was sub-cultured in 10 mL TSB with 0.5 mM $CaCl_2$ at an OD_{600} of 0.1 and the culture was grown at 37ºC to an OD_{600} of 0.7-1.0. Dilutions of the donor phage lysate were prepared in phage buffer. Then, 600 μL *S. aureus* was spun down

(19,000 × g for 2 min) for each dilution of phage, the supernatant was removed, and pellets were resuspended in 600 µL phage dilution. No bacteria (phage only) and no phage controls were run to ensure sterility. After a 5 min incubation at RT, 1.5 mL TSB with 0.5 mM $CaCl_2$ was added to the phage-bacteria mix and samples were incubated at 37 ºC for 20 min. Then, 1 mL of 2 mM sodium citrate was added to stop the reaction and samples were centrifuged at 3,000 × g for 15 min. Pellets were resuspended in 100 µL 0.2 mM sodium citrate and plated on TSA plates containing 2 mM sodium citrate and the antibiotic to select for the desired mutation. Plates were incubated at 37 ºC for at least 24 h, then colonies were screened for the desired mutation.

2.4 Cloning and mutagenesis of *S. aureus*

2.4.1 Complementation of the *hemB*::Sp mutant

The *hemB* gene was PCR amplified using Phusion polymerase, *S. aureus* USA300 genomic DNA as template, and the *hemB*-F-SacI and *hemB*-R-KpnI primer pair (Table 2), designed for cloning the *hemB* gene into pALC2073. The resulting 999 base pair PCR product and pALC2073 were restriction digested with SacI and KpnI. Then, an enzymatic purification was performed and the *hemB* PCR product and pALC2073 were ligated with T4 ligase. The ligation mixture was transformed into *E. coli* DH5α and transformants were selected on LB agar containing ampicillin. *E. coli* colonies carrying plasmids encoding the *hemB* gene were identified through colony PCR using the *hemB* forward and reverse primers.

Plasmids with the correct insert were isolated from *E. coli* and subjected to restriction analysis to verify the presence of the *hemB* gene and the size of the cloned DNA fragment. Three randomly selected plasmids encoding *hemB* were transformed into *S. aureus* RN4220 by electroporation. Plasmids modified by *S. aureus* RN4220 were then extracted and transformed by electroporation into the *hemB*::Sp mutant. In parallel, the *hemB*::Sp mutant was also transformed with the empty vector control pALC2073. Transformants showing *hemB* complementation were selected for by resistance to chloramphenicol and for having an increased colony size compared to transformants carrying empty pALC2073.

2.4.2 Construction of a *S. aureus* mutant dependent on TCA cycle citrate for staphyloferrin biosynthesis

An in-frame, markerless deletion of *sbnG* in the USA300 *sfa*::Km mutant was generated using pKOR1Δ*sbnG*, as previously described[92,133]. Briefly, pKOR1Δ*sbnG* plasmid DNA was isolated from RN4220(pKOR1Δ*sbnG*) grown overnight at 30˚C in TSB with chloramphenicol. The plasmid was introduced into the recipient strain, USA300 *sfa*::Km, by electroporation. USA300 *sfa*::Km(pKOR1Δ*sbnG*) was grown overnight in TSB with chloramphenicol at 30˚C, sub-cultured the next day and grown for 6 h at 30˚C, and then overnight at 42˚C. Dilutions of the overnight culture were plated on TSA plates containing chloramphenicol and incubated overnight at 42˚C. From these plates, 2-3 of the large colonies were picked and grown overnight at 30˚C in a single tube of TSB without antibiotics. The next day, this culture was diluted and plated on TSA plates containing anhydrotetracycline (250 ng/mL). Plates were incubated at 30˚C, and the big colonies that arose were patched onto TSA plates with and without chloramphenicol. Successful USA300 *sfa*::Km Δ*sbnG* mutants were screened through sensitivity to chloramphenicol, which indicated loss of the pKOR1 backbone, and confirmed through PCR, using Taq polymerase and the *sbnG* primer pair (Table 2).

2.4.3 Generation of *hemB*::Sp staphyloferrin biosynthetic and uptake mutants

To generate *hemB*::Sp staphyloferrin biosynthetic and uptake mutants, several phage transductions were performed. Specifically, a *hemB*::Sp donor phage lysate was prepared from USA300 *hemB*::Sp and this donor lysate was used to transduce the *hemB*::Sp mutation into the USA300 *sfa*::Km, USA300 *sbn*::Tc, USA300 *sfa*::Km *sbn*::Tc, USA300 Δ*hts*, and USA300 *sfa*::Km Δ*sbnG* recipient backgrounds. To screen for the *hemB*::Sp mutation, colonies with resistance to spectinomycin, small colony size, and increased growth on TSA plates supplemented with 2 µM hemin were selected for, since disruption of *hemB*::Sp was shown to generate an SCV (section 3.1). To generate the *hemB*::Sp *sirA*::Km mutant, a donor phage lysate had to be prepared from *S. aureus* Newman *sirA*::Km. The *sirA*::Km donor phage lysate was prepared and used to transduce the *sirA*::Km mutation into the USA300 *hemB*::Sp recipient background. Colonies were screened by resistance to kanamycin. Confirmation of all the transduction mutants was through PCR, using Taq polymerase and the respective primer pair (Table 2).

2.5 Preparation of hemin

Hemin stocks were prepared by dissolving 0.0033 g/mL bovine hemin (Sigma) in 0.1 N NaOH. The solution was diluted 1000-fold in 0.1 N NaOH, and the absorbance at 385 nm (A_{385}) was determined. To determine the concentration of the hemin stock, the molar extinction coefficient for hemin in 0.1 N NaOH at 385 nm (58400 cm^{-1} M^{-1}) was used. The hemin stock was sterilized by filtration through a 0.2 µm filter. Hemin aliquots of either 10 µL or 100 µL were prepared and frozen at -20˚C. Before use, 10 µL hemin stocks were diluted 1:10 by addition of 90 µL of the growth medium.

2.6 Growth assays

2.6.1 TSB growth assays

Growth of the *hemB*::Sp mutant relative to WT (carrying the empty vector pALC) and *hemB*::Sp p*hemB* was assessed in TSB, a rich growth medium. Single isolated colonies were picked from TSA plates and used to inoculate 5 mL TSB tubes. Overnight cultures of bacteria were washed twice with sterile 0.9% (w/v) saline and normalized to an OD_{600} of 0.1. TSB tubes were inoculated with diluted *S. aureus* to give a starting OD_{600} of 0.001. After 24 h of incubation, bacterial growth was assessed by measuring the endpoint OD_{600}.

2.6.2 Assessment of hemin auxotrophy on TSA plates

Phenotypic assessment of the *hemB*::Sp mutant, relative to WT USA300 (carrying the empty vector pALC) and the *hemB*-complemented strain (containing p*hemB*) was performed on TSA plates supplemented with either 0 µM or 2 µM hemin. Briefly, single isolated colonies were picked from TSA plates and used to inoculate 5 mL TSB tubes. Overnight cultures of bacteria were washed twice with sterile 0.9% (w/v) saline and normalized to an OD_{600} of 0.1. This resuspension was serially diluted 10-fold through to 10^{-4} and 10 µL of each dilution was drop plated on TSA plates with either 0 µM or 2 µM hemin. Plates were incubated at 37°C for 48 h and representative images were taken.

2.6.3 TMS growth assays

For initial growth assessment of the *hemB*::Sp mutant relative to WT and the *hemB*-complemented strain (containing p*hemB*) in the minimal media TMS, single colonies were picked from TSA plates and grown overnight in TSB. Overnight cultures of bacteria were washed twice with sterile 0.9% (w/v) saline and normalized to an OD_{600} of 0.1. Next, 14 mL round-bottom polypropylene tubes with 1 mL TMS were inoculated with diluted *S. aureus* to give a starting OD_{600} of 0.001. After 24 h of incubation, bacterial growth was assessed by measuring the endpoint OD_{600}.

All subsequent TMS growth assays were performed as described above, with the exception that TMS was supplemented with a minimal amount of hemin (0.2-0.4 µM hemin), unless otherwise indicated, to enable growth of *hemB*::Sp SCV bacteria. The amount of hemin added to media was specified for each experiment. Moreover, in all future experiments, overnight cultures were grown in TMS supplemented with minimal hemin rather than TSB.

Where specified, Tris-maleic acid buffered TMS at pH 7.4 or pH 6.0 was used in place of regular TMS. Briefly, TMS was prepared as described, except 6.05 g Tris base and 450 mL H_2O was replaced with an equal volume of Tris-maleic acid buffer (6.06 g Tris base and 5.80 g maleic acid dissolved in 500 mL H_2O).

2.6.4 Bacterial growth curves

Growth of the *hemB*::Sp mutant over time relative to WT (carrying the empty vector pALC) and the *hemB*-complemented strain (containing p*hemB*) was assessed in TMS supplemented with 0.2 µM hemin. Bacteria were prepared in the same way as with the TMS growth assays and TMS was inoculated to give a starting OD_{600} of 0.001, but rather than incubating cultures in 14 mL round-bottom polypropylene tubes, three 200 µL aliquots for each biological replicate were prepared. Cultures were grown in a Bioscreen C machine (Growth Curves USA, Piscataway, NJ) at 37°C with continuous shaking at medium amplitude, and OD_{600} was measured every 30 min for 48 h. For graphical clarity, bacterial growth was illustrated at 4 h intervals for the first 24 h.

2.6.5 Assessment of siderophore utilization

To assess siderophore utilization of *hemB*::Sp bacteria, an iron restricted condition had to be established in TMS supplemented with minimal hemin. Fetal bovine serum (FBS; Wisent) and horse serum (HS; Sigma), heat inactivated by incubation at 55˚C for 1 h, and human apo-Tfn

(Sigma) were assessed for their ability to restrict iron in TMS. Iron restriction in media was alleviated by the addition of ferrous ammonium sulfate (FAS; VWR), which was a source of free Fe^{3+} or Fe^{2+} (at pH 7.4 or 6.0, respectively). Moreover, to assess the ability of *S. aureus hemB*::Sp bacteria to utilize siderophores, SA (Indus Biosciences Private Limited), DFO (Hospira; obtained from the London Health Sciences Centre), or epinephrine (Sigma) were added to iron restricted media. The concentration of iron-restricting agent, FAS, and siderophore added was specified for each experiment.

2.7 Western blots

To examine expression of *S. aureus* siderophore-binding lipoproteins SirA, HtsA, and $FhuD_2$ by *hemB*::Sp bacteria, Western blot analyses were performed. *S. aureus* strains were grown overnight in TMS supplemented with minimal hemin, overnight cultures were washed twice with 0.9% (w/v) saline, normalized, and used to inoculate 3 mL TMS supplemented with minimal hemin and either additional Fe^{3+} (in the form of FAS) or Tfn to give an initial OD_{600} of 0.001. Cultures were grown for 24 h, normalized to an OD_{600} of 1.0, and pelleted by centrifugation (19,000 × g for 2 min). To prepare cell lysates, bacterial pellets were resuspended in 75 µL LBL and incubated at 37˚C for 1 h. After lysis, 25 µL 4 x Laemmli buffer (240 mM Tris-HCl, pH 6.8, 8% (w/v) SDS, 40% (v/v) glycerol, 0.04% (w/v) bromophenol blue) was added and *S. aureus* samples were boiled for 10 min. Proteins were separated by SDS-polyacrylamide gel electrophoresis (SDS-PAGE) on a 12% polyacrylamide gel. After electrophoresis, standard protocols were followed to transfer proteins to a nitrocellulose membrane. The membrane was blocked with 8% (w/v) skim milk for 3 h before addition of primary antibody (rabbit anti-SirA, rabbit anti-HtsA, or rabbit anti-$FhuD_2$ antiserum (diluted 1:1000)). Membranes were incubated with primary antibody overnight at 4˚C before addition of secondary antibody (donkey anti-rabbit IgG antibody, DyLight 800 conjugated (diluted 1:20,000); Rockland Immunochemicals, Inc., Limerick, PA). An Odyssey CLx Imaging System and LI-COR Image Studio 4.0 software (LI-COR Biosciences) were used to image the membranes.

2.8 Murine model of systemic infection

All animal experiments were performed in compliance with guidelines set out by the Canadian Council on Animal Care. All animal protocols (#2017-028) were reviewed and approved by the University of Western Ontario Animal Use Subcommittee, a subcommittee of the University

Council on Animal Care. Six-week-old female BALB/c mice (Charles River laboratories) were injected via tail vein with 100 µL of bacterial culture, containing approximately $7 \times 10^6 – 1 \times 10^7$ colony-forming units (CFU) of *S. aureus* bacteria. To prepare the bacteria, strains were grown to OD_{600} 2-2.5 in TSB, washed twice with phosphate buffered saline (PBS) and resuspended to OD_{600} 0.2 in PBS, corresponding to a cell density of approximately $7 \times 10^7 – 1 \times 10^8$ CFU/mL. Mice were weighed at the time of infection and infections were allowed to proceed for 48 h before animals were euthanized, reweighed, and organs were aseptically harvested in ice-cold PBS + 0.1% (v/v) Triton X-100 (Thermo Fischer Scientific). Extracted organs were homogenised in a Bullet Blender Storm (Next Advance, Troy, NY) using metal beads, serially diluted, and plated on TSA for enumeration of bacterial burden, presented as $\log_{10}$ CFU per organ.

For animal experiments involving DFO treatment, 100 µL of a 10 mg/mL solution of DFO (suspended in sterile PBS) were administered intraperitoneally, one dose at the time of bacterial challenge, and a second dose 24 h post-infection. For the no treatment group, 100 µL PBS (vehicle control) was administered intraperitoneally, in parallel to DFO injection. The dose of DFO administered over the course of the two first days of infection was the same as previously employed by Arifin *et. al*[99] and corresponded to approximately 50 mg/kg/day which is comparable to the weight-adjusted dose recommended for use in humans (Hospira).

2.9 Statistical analysis

All statistical analyses and graph production were performed using GraphPad Prism software (GraphPad Software, La Jolla, CA).

Chapter 3

3 Results

3.1 The *S. aureus* USA300 *hemB*::Sp mutant is a stable SCV that is auxotrophic for hemin.

To investigate the iron acquisition strategies employed by *S. aureus* SCVs, it was necessary to genetically engineer a stable SCV because clinically isolated SCV strains are known to spontaneously revert to WT state[103]. Clinical SCVs are often auxotrophic for hemin, thus have deficient electron transport[103]. Previous studies have shown that genetic mutation of *hemB* in *S. aureus* generates the electron-transport-deficient SCV phenotype[113]. *S. aureus hemB* mutants have been utilized by various research groups to study aspects of SCV pathogenesis, such as intracellular survival[113]. Therefore, I employed the *S. aureus* USA300 *hemB*::Sp mutant to study *S. aureus* SCV iron acquisition strategies. First, I characterized *in vitro* growth of the *hemB*::Sp mutant to confirm that it is indeed a SCV that is auxotrophic for hemin. When grown in liquid TSB, a nutrient rich medium, the *hemB*::Sp mutant grew after 24 h, however growth was significantly reduced compared to WT, *S. aureus* USA300 (Fig. 3A). Provision of *hemB in trans*, on the plasmid p*hemB*, restored growth of *hemB*::Sp bacteria to WT levels, irrespective of the growth medium (Fig. 3). When grown on TSA, *hemB*::Sp bacteria formed slow-growing colonies that were smaller in size and less pigmented when compared to WT colonies, characteristic of electron-transport-deficient SCVs (Fig. 3B). Importantly, providing *hemB*::Sp bacteria with additional hemin increased colony size and restored colony pigmentation of the SCV bacteria, indicating that *hemB*::Sp bacteria are indeed auxotrophic for hemin (Fig. 3B).

To study the iron acquisition strategies employed by *S. aureus*, the Heinrichs lab often uses the minimal medium TMS because iron content can be controlled[91,92,99,134]. As expected, WT grew in TMS but the *hemB*::Sp mutant was unable to grow, indicating that TMS lacks sufficient hemin to support growth of a hemin auxotroph (Fig. 3C). Therefore a condition that could allow *hemB*::Sp bacteria to grow yet still behave as an SCV as compared to WT bacteria (i.e. demonstrate reduced growth) had to be established to permit characterization of SCV iron acquisition mechanisms. Supplementation of TMS with a minimal concentration of hemin of 0.2 µM was found to permit slow growth of *hemB*::Sp, however this hemin concentration did not restore growth to WT levels, indicated by the early plateau of the growth curve after 24 h (Fig. 3D). Therefore, the *S. aureus*

hemB::Sp mutant is a SCV that is auxotrophic for hemin, and a condition in TMS was established for growth of *hemB*::Sp.

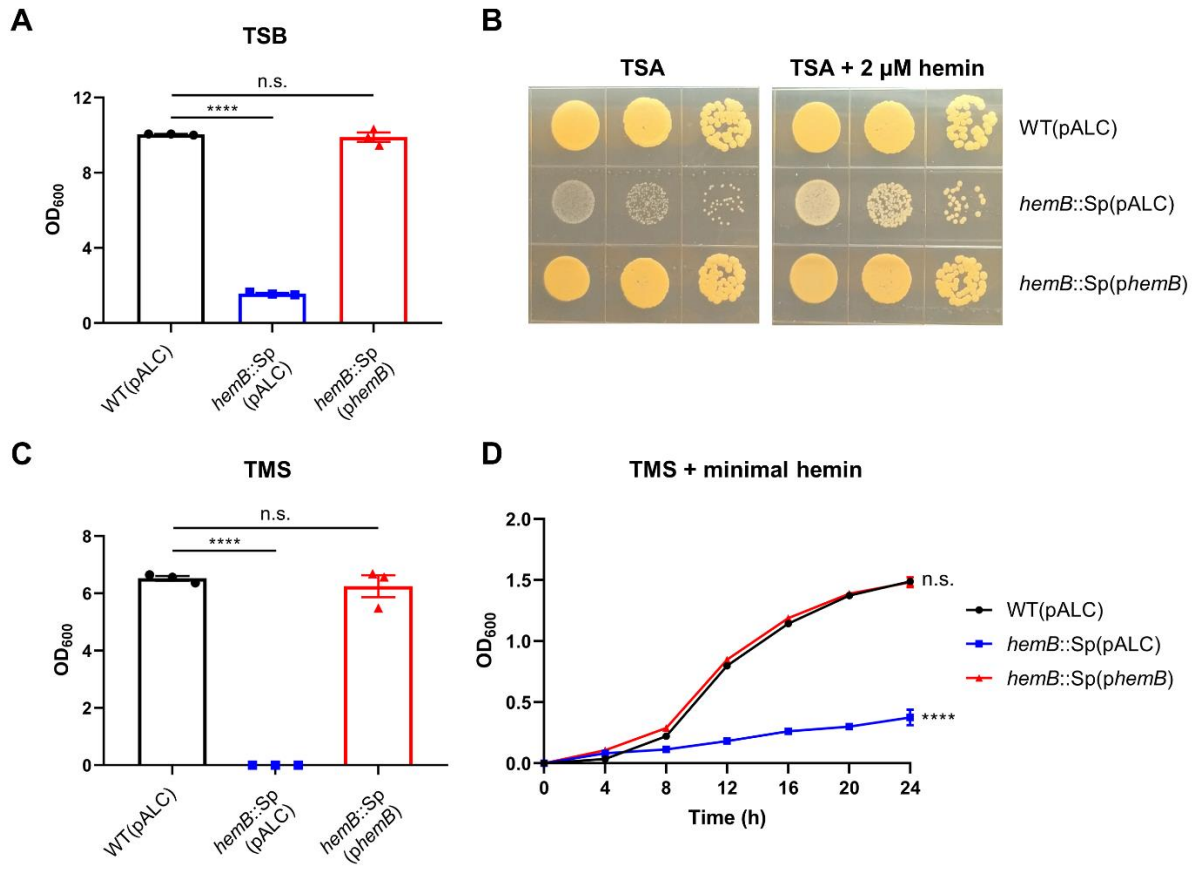

Figure 3. *S. aureus hemB*::Sp is a SCV auxotrophic for hemin. (A) Growth in TSB after 24 h. **(B)** Representative image depicting growth on TSA plates without hemin or with 2 µM hemin after 48 h. **(C)** Growth in TMS after 24 h. **(D)** Growth over 24 h in TMS supplemented with 0.2 µM hemin. Data are plotted as mean ± SEM, three biological replicates. Three measurements per replicate were performed in (D). **** $p<0.0001$, one-way ANOVA with Tukey's post test (A, C), two-way ANOVA with Tukey's post test (D).

3.2 Growth promotion and restriction of the *S. aureus hemB*::Sp mutant by two different sera.

Next, I sought to establish an iron restricted growth condition to allow the study of iron acquisition mechanisms utilized by *S. aureus* SCVs. Previous studies characterizing iron acquisition in *S.*

aureus have routinely used serum, which contains transferrin, to restrict iron availability[91,130]. Therefore, I examined the ability of fetal bovine serum (FBS) and horse serum (HS) to restrict iron when added to TMS supplemented with a minimal amount of hemin. These experiments revealed that there was a massive difference between the sera, as the addition of 20% (v/v) FBS improved growth of *hemB*::Sp bacteria to WT levels, but the addition of 20% (v/v) HS completely abolished growth of *hemB*::Sp bacteria (Fig. 4A). In all the conditions tested, *hemB*::Sp bacteria carrying the p*hemB* complementation plasmid grew the same as WT indicating that the observed defects were *hemB*-dependent (Fig. 4A). FBS was without effect on the growth of WT and *hemB*::Sp(p*hemB*) *S. aureus*, while HS reduced growth (Fig. 4A). Previous work by the Heinrichs lab has shown that a *S. aureus sfa*::Km *sbn*::Tc mutant, deficient for SA and SB biosynthesis, has a severe growth defect in iron-restricted media[91,92]. Therefore, I employed this staphyloferrin deficient mutant as a control for my study as impaired growth of this strain would indicate the media is indeed iron restricted. As expected, growth of the staphyloferrin deficient mutant was abolished upon addition of 20% (v/v) HS to TMS supplemented with minimal hemin (Fig. 4B). Importantly, when Fe^{3+} in the form of FAS was added to media containing HS, growth of the staphyloferrin deficient strain was completely restored, indicating the growth defect was indeed due to iron starvation (Fig. 4B). Interestingly, growth of the *hemB*::Sp SCV was also abolished in HS, however Fe^{3+} did not restore growth (Fig. 4B). To determine whether the attenuated growth of the *hemB*::Sp mutant in the iron restricted condition was due to limited iron availability rather than a contaminant within HS, growth of *hemB*::Sp bacteria in neutral and acidic media was compared. At neutral pH, iron exists in the Fe^{3+} oxidized state which is readily bound by serum transferrin whereas at acidic pH iron is reduced to the Fe^{2+} state which does not bind transferrin. Interestingly, at neutral (pH 7.4) and acidic (pH 6.0) pH, growth of *hemB*::Sp bacteria in TMS supplemented with 0.2 µM hemin and HS was significantly impaired (Fig. 4C). Moreover, growth was not improved upon addition of iron to the media (Fig. 4C). Taken together, these data indicate that a factor other than iron restriction was suppressing growth of *hemB*::Sp bacteria in a HS dependent manner. Therefore, while HS has previously been used in the Heinrichs lab to restrict iron[91,130], it was not suitable for growth analyses of *hemB*::Sp SCV bacteria.

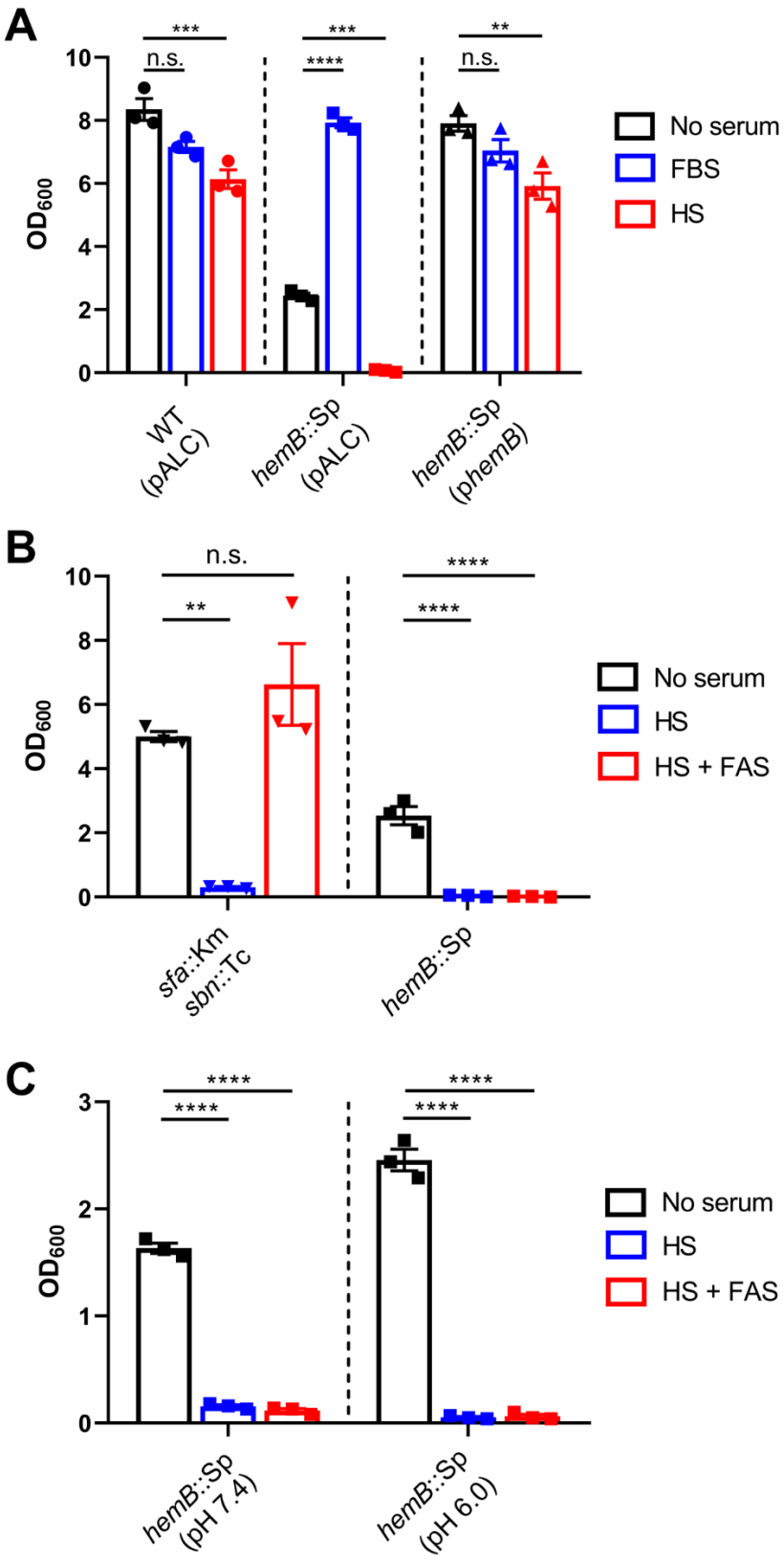
A
***
n.s.
***
****
**
n.s.
10
8
6
4
2
0
OD600
No serum
FBS
HS
WT (pALC)
hemB::Sp (pALC)
hemB::Sp (phemB)
B
n.s.
**
****
****
10
8
6
4
2
0
OD600
No serum
HS
HS + FAS
sfa::Km sbn::Tc
hemB::Sp
C
****
****
****
****
3
2
1
0
OD600
No serum
HS
HS + FAS
hemB::Sp (pH 7.4)
hemB::Sp (pH 6.0)

Figure 4. Growth of *hemB*::Sp bacteria in media containing serum. Growth in TMS supplemented with 0.2 µM hemin after 24 h. **(A)** No serum, 20% (v/v) FBS, or 20% (v/v) HS was added to the media. **(B)** No serum, 20% (v/v) HS, or 20% (v/v) HS and 10 µM FAS was added to the media. **(C)** Tris-maleic acid buffered TMS at pH 7.4 or pH 6.0 was used in place of regular TMS. No serum, 20% (v/v) HS, or 20% (v/v) HS and 10 µM FAS was added to the media. Data are plotted as mean ± SEM, three biological replicates. ** $p<0.01$, *** $p<0.001$, **** $p<0.0001$, one-way ANOVA with Tukey's post test.

3.3 Transferrin restricts growth of the *S. aureus hemB*::Sp mutant in an iron-dependent manner.

To study the iron acquisition strategies of *S. aureus* SCVs, suitable iron restricted conditions needed to be established. Therefore, I assessed the ability of purified Tfn to restrict iron in TMS supplemented with minimal hemin. Through titration of the amount of Tfn added to the culture medium, I established that 1.25 µM Tfn was the minimal amount of Tfn that could abolish growth of siderophore deficient *S. aureus*, which served as a positive control to indicate iron restriction (Fig. 5A-B). Importantly, growth of the staphyloferrin mutant was recovered upon addition of Fe^{3+} to the iron-restricted medium (Fig. 5B). Growth of the *hemB*::Sp mutant was also significantly reduced upon Tfn addition however growth was not restored upon addition of free Fe^{3+} (Fig. 5B). Given that 0.2 µM hemin was the absolute minimum concentration of hemin required for growth of *hemB*::Sp bacteria in TMS, it was possible that Tfn or a contaminant of Tfn affected the ability of *hemB*::Sp bacteria to attain this critical nutrient, thereby impeding growth of the hemin auxotroph. To test this notion, the concentration of hemin used to supplement TMS was increased 2-fold from 0.2 µM to 0.4 µM hemin, and growth was reassessed. Under these conditions, the *hemB*::Sp mutant still grew poorly as compared to non-SCV *S. aureus* in the absence of Tfn, indicating 0.4 µM hemin can be used to permit SCV growth without completely complementing the hemin auxotrophy (Fig. 5C). Using these conditions, growth of *hemB*::Sp bacteria was restricted when Tfn was added and excess Fe^{3+} fully restored *hemB*::Sp growth (Fig. 5C). Importantly, staphyloferrin deficient *S. aureus* remained unable to grow in TMS supplemented with 0.4 µM hemin and Tfn unless excess Fe^{3+} was added (Fig. 5C). Therefore, Tfn-dependent iron depleted growth conditions, to permit characterization of iron acquisition systems in SCV bacteria, were established.

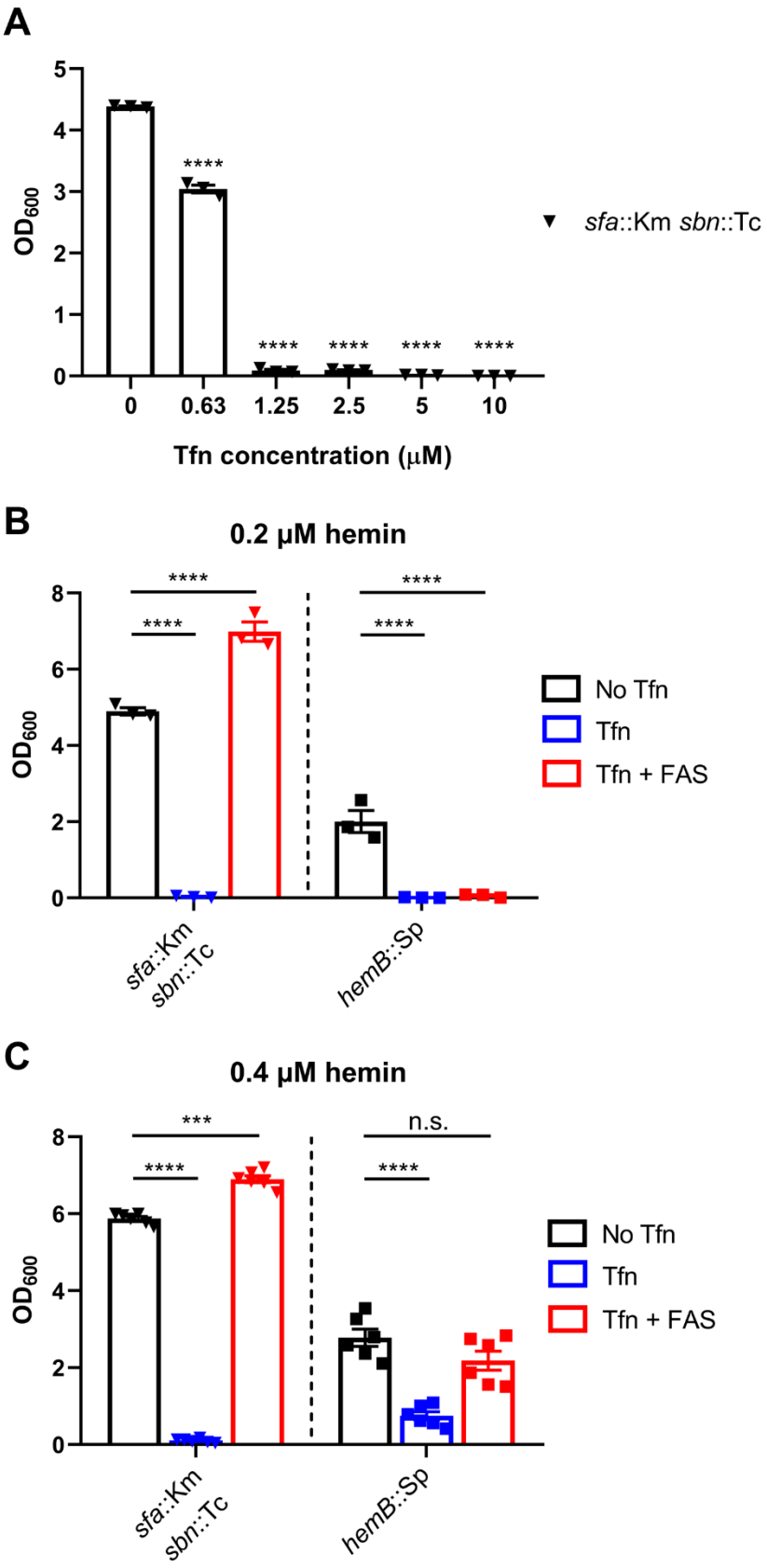
A
OD600
Tfn concentration (μM)
0
0.63
1.25
2.5
5
10
****
sfa::Km sbn::Tc
B
0.2 μM hemin
OD600
No Tfn
Tfn
Tfn + FAS
sfa::Km sbn::Tc
hemB::Sp
C
0.4 μM hemin
***
n.s.

Figure 5. Growth of the *hemB*::Sp mutant in media containing Tfn. (A) Growth of staphyloferrin deficient *S. aureus* in TMS supplemented with 0.2 µM hemin and increasing concentrations of Tfn after 24 h. **(B-C)** Growth in TMS after 24 h with 0.2 µM hemin (B) or 0.4 µM hemin (C). No Tfn, 1.5 µM Tfn, or 1.5 µM Tfn and 10 µM FAS was added to the media. Data are plotted as mean ± SEM, three biological replicates (A, B) or six biological replicates (C). *** $p<0.001$, **** $p<0.0001$, one-way ANOVA with Tukey's post test.

3.4 The *hemB*::Sp mutant uses SB but not SA to support its growth in iron deplete media.

Having established the appropriate culture conditions, I next compared the growth of WT *S. aureus* to the *hemB*::Sp mutant and the complemented strain under iron depleted conditions. This analysis revealed that in media supplemented with 0.4 µM hemin, the *hemB*::Sp mutant displayed reduced growth relative to WT and the complemented strain in the absence of transferrin (Fig. 6). In the presence of transferrin, WT *S. aureus* retained most of its ability to proliferate, whereas *hemB*::Sp bacteria demonstrated a 3-fold growth reduction compared to the no Tfn condition (Fig. 6). The complemented strain *hemB*::Sp(p*hemB*) grew comparable to WT in all conditions examined (Fig. 6). Interestingly, under conditions of iron restriction, growth of *hemB*::Sp bacteria was reduced but not completely abolished (Fig. 6). The addition of excess Fe^{3+} in the form of FAS restored the growth of each strain to the no Tfn condition, indicating the apparent growth defects were due to iron restriction (Fig. 6). In each experiment, the *sfa*::Km *sbn*::Tc mutant was employed as a positive control strain that would show growth defects under iron restriction. Use of this mutant revealed that SA and/or SB production was essential for *S. aureus* growth in iron deplete media, as demonstrated by the inability of this strain to grow in the presence of Tfn (Fig. 6). Furthermore, the fact that the *hemB*::Sp mutant grows in in the presence of Tfn, albeit to reduced levels, suggests this SCV must produce SA and/or SB to support the level of growth achieved (Fig. 6).

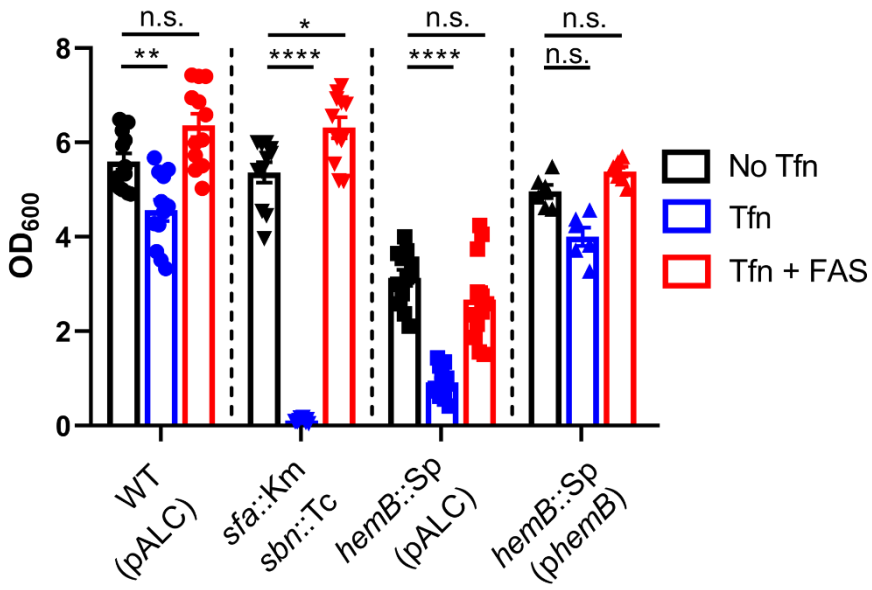

Figure 6. Growth of *hemB*::Sp in iron deplete media. Growth in TMS supplemented with 0.4 µM hemin after 24 h. No Tfn, 1.5 µM Tfn, or 1.5 µM Tfn and 10 µM FAS was added to the media. Data are plotted as mean ± SEM, at least six biological replicates. * $p<0.05$, ** $p<0.01$, **** $p<0.0001$, one-way ANOVA with Tukey's post test.

To investigate whether *hemB* deficient *S. aureus* utilizes SA and/or SB, I generated single and double mutants of the SA and SB biosynthetic loci, *sfa* and *sbn*, respectively, in the *hemB*::Sp mutant background. Growth of *hemB*::Sp single and double staphyloferrin biosynthetic mutants was examined in the established iron restricted condition. Mutation of staphyloferrin biosynthesis in the *hemB*::Sp background did not affect growth in media where iron was freely available (Fig. 7A). In contrast, mutation of both staphyloferrin biosynthetic loci in the *hemB*::Sp background eliminated growth under iron restricted conditions, consistent with the idea that *hemB S. aureus* makes siderophore (Fig. 7A). Interestingly, SA deficient *hemB*::Sp mutants displayed no growth defect relative to parental *hemB*::Sp. In contrast, SB deficient *hemB*::Sp bacteria were attenuated for growth under iron restricted conditions and displayed the same level of growth as the siderophore deficient *hemB* strain (Fig. 7A). From these observations, it can be inferred that SA biosynthesis and/or utilization is insufficient to support growth of *hemB*::Sp when iron is limited. Conversely, these data indicate that SB must enable *hemB*::Sp bacteria to acquire iron and sustain growth when free iron is not readily available.

To examine whether *hemB*::Sp bacteria express the SirA receptor required for SB utilization in a Fur-dependent manner, I performed Western blots assessing SirA expression. When iron is freely available, SirA expression by *S. aureus* is downregulated by Fur, however, expression of SirA is upregulated in conditions where iron is restricted which enables SB utilization. Therefore, I prepared whole cell lysates of *S. aureus* grown in TMS supplemented with either iron in the form of FAS or Tfn, where expression of SirA should be minimal or significantly upregulated, respectively. *S. aureus* Newman (NWMN) and an isogenic *sirA*::Km mutant served as positive and negative controls, respectively, for expression of SirA (Fig. 7D). Western blots were performed using anti-SirA antiserum and demonstrated that WT, *hemB*::Sp and *hemB*::Sp(p*hemB*) *S. aureus* all expressed SirA in an iron-dependent manner, as indicated by increased protein from bacteria grown in the iron-starved (Tfn) condition (Fig. 7D). Thus, Fur-dependent gene regulation of SirA was normal in a *S. aureus hemB*::Sp mutant, which is required for SB utilization.

To further investigate SA and SB utilization by *hemB*::Sp bacteria, mutagenesis of the dedicated SA uptake locus and SB receptor, *hts* and *sirA*, respectively, was performed in the *hemB*::Sp mutant background to create SCV strains that can either not utilize SA or that cannot utilize SB. Under iron replete conditions, the *hemB*::Sp mutants deficient for staphyloferrin utilization grew similar to parental *hemB*::Sp bacteria (Fig. 7B). In contrast, under conditions of iron restriction inactivation of *sirA*, which would render *hemB*::Sp *S. aureus* unable to utilize SB, abolished growth of *hemB*::Sp while inactivation of the *hts* operon required for SA utilization was without effect (Fig. 7B). Moreover, mutation of SA uptake did not affect growth of *hemB*::Sp bacteria in the iron deplete condition (Fig. 7B). These observations are consistent with the interpretation of the data presented in Fig. 5A and indicate that *hemB* deficient *S. aureus* utilize SB and not SA for growth when iron was depleted in the medium. To ensure that SCV bacteria were not growing to WT levels and that iron was restricted when Tfn was added, WT *S. aureus* and the siderophore deficient mutant were again used as controls (Fig. 7C). Indeed, growth of non-SCV bacteria was approximately double that of SCV bacteria, and growth of the *S. aureus* siderophore deficient mutant was abolished when iron was restricted (Fig. 7A-C). Taken together, these data provide strong evidence that the *hemB*::Sp mutant has a defect in SA utilization, and relies on SB alone to support growth where iron is not freely available.

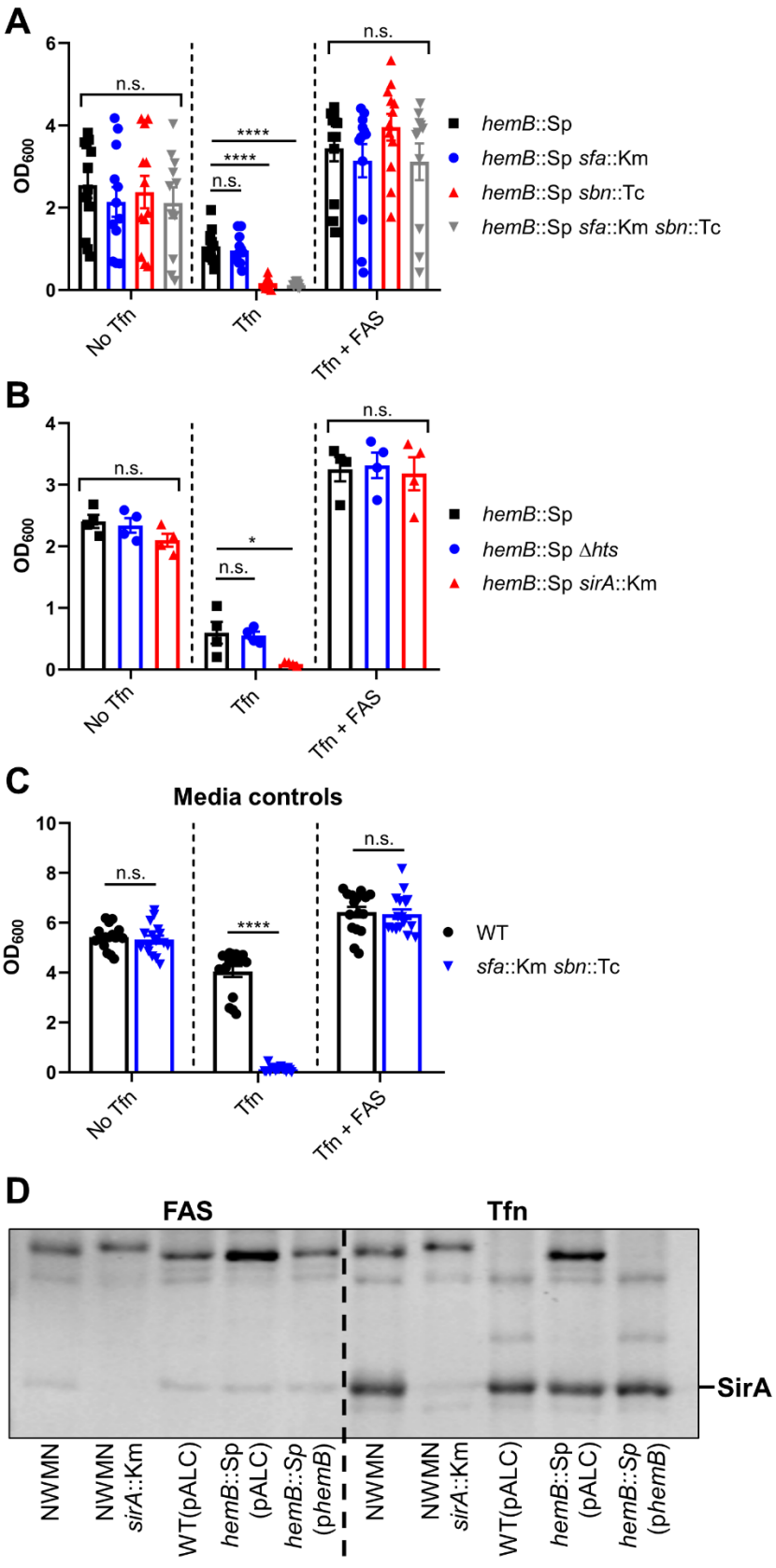
A
OD600
n.s.
****
****
n.s.
n.s.
No Tfn
Tfn
Tfn + FAS
hemB::Sp
hemB::Sp sfa::Km
hemB::Sp sbn::Tc
hemB::Sp sfa::Km sbn::Tc
B
OD600
n.s.
*
n.s.
n.s.
No Tfn
Tfn
Tfn + FAS
hemB::Sp
hemB::Sp Δhts
hemB::Sp sirA::Km
C
Media controls
OD600
n.s.
****
n.s.
No Tfn
Tfn
Tfn + FAS
WT
sfa::Km sbn::Tc
D
FAS
Tfn
SirA
NWMN
NWMN sirA::Km
WT(pALC)
hemB::Sp (pALC)
hemB::Sp (phemB)
NWMN
NWMN sirA::Km
WT(pALC)
hemB::Sp (pALC)
hemB::Sp (phemB)

Figure 7. *hemB*::Sp uses SB to support growth in iron deplete media. (A-C) Growth in TMS supplemented with 0.4 µM hemin after 24 h. No Tfn, 1.5 µM Tfn, or 1.5 µM Tfn and 10 µM FAS was added to the media. Data are plotted as mean ± SEM of twelve (A), four (B), or sixteen (C) biological replicates. **** $p<0.0001$, one-way ANOVA with Tukey's post test. **(D)** Western blot for detection of SirA (37 kDa) in whole cell lysates prepared from cultures grown for 24 h in TMS supplemented with 0.4 µM hemin and either FAS (30 µM) or Tfn (1.5 µM).

3.5 *S. aureus hemB*::Sp bacteria can utilize exogenously provided SA.

Given that the growth data presented above indicated that the *hemB*::Sp mutant had a defect in SA utilization, I next investigated the mechanisms underlying this defect. First, I examined the expression of HtsA, the Fur-regulated SA receptor required for uptake[81], in *hemB*::Sp bacteria. To test this, Western blots of whole cell lysates from bacteria that were grown in media with excess iron or Tfn were probed with anti-HtsA antiserum. A Δ*hts* mutant was employed as a negative control for expression of HtsA (Fig. 8A). Comparable to the Western blot for SirA expression, WT *S. aureus* expressed HtsA in an iron-dependent manner, indicated by an increase protein when iron was restricted in the medium by Tfn (Fig. 8A). Notably, the *hemB*::Sp and *hemB*::Sp(p*hemB*) mutants also displayed normal Fur-regulated expression of HtsA (Fig. 8A). Therefore, it is unlikely that SA uptake is defective in *hemB*::Sp bacteria.

To test directly whether *hemB*::Sp bacteria can indeed take up SA, growth experiments were performed as previously described, however, purified SA was also added to media containing Tfn and growth was analyzed. As previously shown, growth of the *hemB*::Sp mutant was significantly reduced in the presence of Tfn, but the SCV still demonstrated growth presumably due to SB utilization (Fig. 8B). Interestingly, the addition of Fe^{3+} restored growth of *hemB*::Sp bacteria back to the levels seen in the absence of Tfn, however the addition of SA was without effect (Fig. 8B). The purified SA was indeed functional, as it completely restored normal growth to siderophore deficient *S. aureus* (Fig. 8B). WT and *hemB*::Sp(p*hemB*) bacteria grew to approximately the same extent in all the conditions (Fig. 8B). To eliminate background SB-dependent growth of *hemB*::Sp bacteria and investigate only SA-dependent growth, *hemB S. aureus* deficient for staphyloferrin biosynthesis was employed. Interestingly, the *hemB*::Sp *sfa*::Km *sbn*::Tc mutant recovered a minimal amount of growth upon addition of SA and reached the same level of growth as *hemB*::Sp bacteria using SB to support growth in the presence of Tfn

(Fig. 8B). These data suggest that SA uptake is not completely defective in *hemB*::Sp bacteria and that dependence on SB for growth in iron deplete media by the *hemB*::Sp mutant was likely due to a defect in SA biosynthesis.

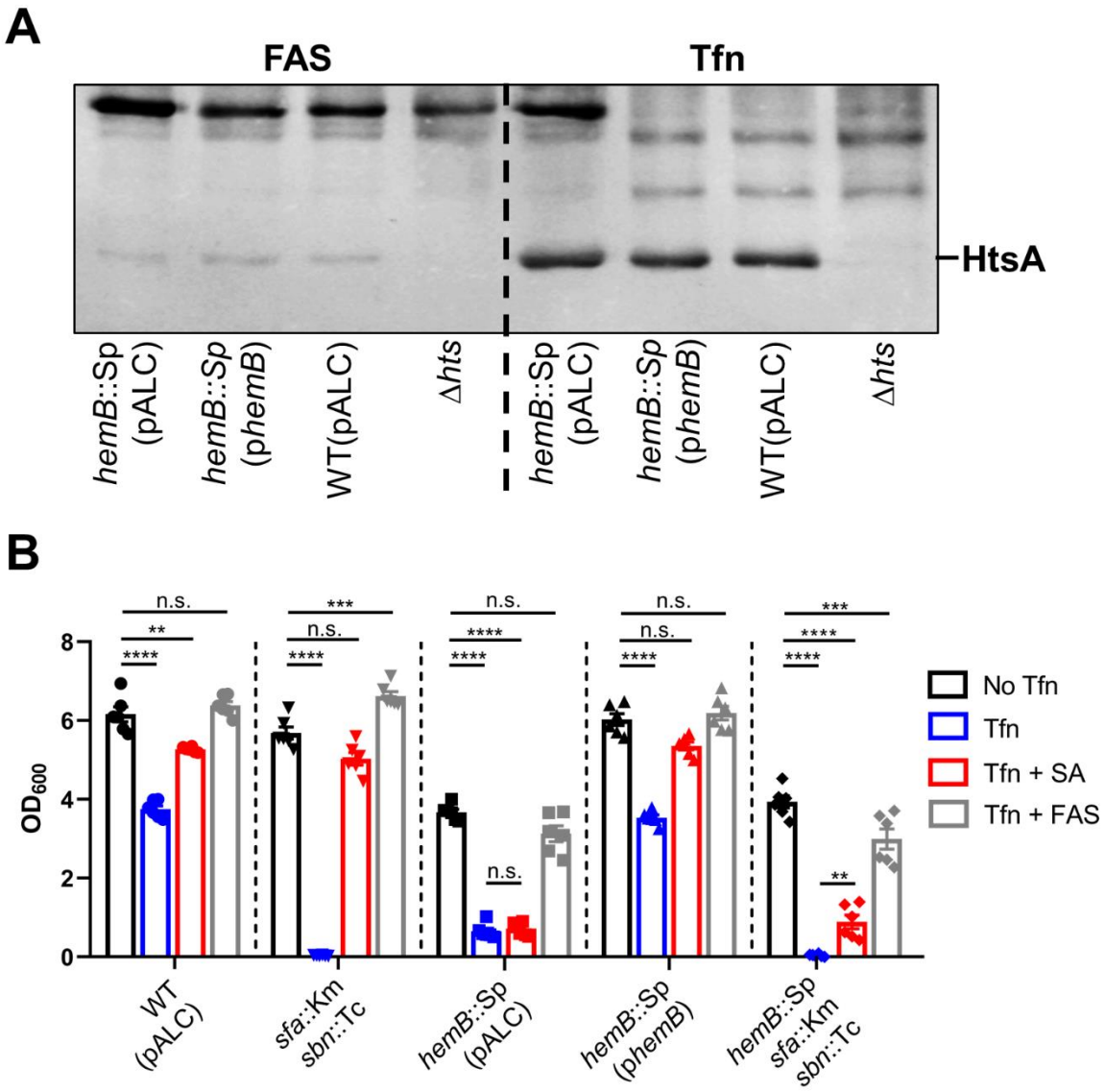

Figure 8. SA utilization by *S. aureus hemB*::Sp. (A) Western blot for detection of HtsA (31 kDa) in whole cell lysates prepared from cultures grown for 24 h in TMS supplemented with 0.4 µM hemin and either FAS (30 µM) or Tfn (1.5 µM). **(B)** Growth in TMS supplemented with 0.4 µM hemin after 24 h. No Tfn, 5 µM Tfn, 5 µM Tfn and 30 µM FAS, or 5 µM Tfn and 100 µM SA was added to the media. Data are plotted as mean ± SEM, six biological replicates. **** p<0.0001, one-way ANOVA with Tukey's post test.

3.6 SB production by *hemB*::Sp bacteria is highly dependent on the SbnG citrate synthase.

I next sought to identify a potential cause for defective SA biosynthesis in *hemB*::Sp *S. aureus*. SA and SB are both comprised of citrate[85,86,135], and previous work by the Heinrichs laboratory has shown that *S. aureus* uses citrate generated by the TCA cycle enzyme citrate synthase CitZ for both SA and SB biosynthesis[92]. Notably, *S. aureus* expresses a second citrate synthase, SbnG, which produces citrate that is incorporated exclusively into SB, but not SA[92]. Thus, TCA cycle activity is essential for generation of SA. Interestingly, the expression of *cit*Z and other TCA cycle genes is downregulated in *hemB*::Sp SCV bacteria[120,121,128]. Therefore, it is likely that downregulation of *citZ* limits the availability of citrate for SA production by *hemB*::Sp bacteria. To determine experimentally whether decreased *citZ* expression causes SA biosynthesis defects, I assessed whether overexpression of *citZ* could improve growth of *hemB*::Sp bacteria where iron is restricted. To do this, I transformed *hemB*::Sp bacteria with the empty vector, pALC2073, or a *citZ* expression vector p*citZ* and analyzed their growth in the presence of Tfn. This analysis revealed that irrespective of the culture conditions there was no difference in growth between these transformants (Fig. 9A). Furthermore, I transformed *hemB*::Sp *S. aureus* deficient for SB with pALC2073 and p*citZ* to eliminate SB-dependent growth of *hemB*::Sp bacteria in iron-restricted media and investigate only how *citZ* expression affects SA-dependent growth. Preliminary data from growth experiments with the resulting SB-deficient transformants revealed that *citZ* provided *in trans* conferred no growth advantage over bacteria carrying the empty vector in iron deplete media (data not shown). Thus, an alternative strategy for determining whether downregulation of *citZ* in electron-transport-deficient *S. aureus* SCVs affects SA biosynthesis had to be examined.

I decided to assess availability of TCA cycle citrate, synthesized by CitZ, for staphyloferrin biosynthesis by generation of *sfa*::Km Δ*sbnG* mutants in the WT and *hemB*::Sp backgrounds. The resulting mutants are entirely dependent on citrate derived from the TCA cycle for generation of SB. If TCA cycle-derived citrate is available, SB synthesis should occur and *sfa*::Km Δ*sbnG* mutants will grow when iron is restricted. In contrast, if TCA cycle citrate is unavailable, *sfa*::Km Δ*sbnG* mutants will not be able to produce SB and will have a growth defect in iron deplete media. Growth of *sfa*::Km Δ*sbnG* and *hemB*::Sp *sfa*::Km Δ*sbnG* was assessed in iron deplete and replete media, as previously described. There was no difference in growth between the non-SCV *sfa*::Km and *sfa*::Km Δ*sbnG* mutants in all the conditions, indicating that TCA cycle-derived citrate was

available for SB biosynthesis and was sufficient to support growth of *sfa*::Km Δ*sbnG* in iron deplete media (Fig. 9B). In contrast, the *hemB*::Sp *sfa*::Km Δ*sbnG* mutant had a significant growth defect relative to the *hemB*::Sp *sfa*::Km mutant in iron-restricted media, which implies defective SB biosynthesis (Fig. 9B). In fact, growth of the *hemB*::Sp *sfa*::Km Δ*sbnG* mutant in the iron deplete condition was not significantly different than growth of *S. aureus* deficient for SA and SB (Fig. 9B). Thus, deletion of *sbnG* in *hemB*::Sp bacteria deficient for SA biosynthesis essentially eliminated SB biosynthesis. These data reiterate that *hemB*::Sp bacteria synthesize SB to support growth in iron deplete media, but demonstrate that SB biosynthesis is highly dependent on citrate generated by SbnG, the second *S. aureus* citrate synthase. Non-SCV *S. aureus* did not require expression of *sbnG* for SB production because CitZ, the TCA cycle citrate synthase, must have generated sufficient citrate for biosynthesis of SB to overcome any deleterious effects of the *sbnG* mutation. Therefore, SCV bacteria presumably have limited CitZ-dependent citrate available for the synthesis of SB. Limited TCA cycle citrate for SB production is an indirect indication of finite citrate for SA production, which requires TCA cycle-derived citrate. Thus, defective SA biosynthesis by *hemB*::Sp bacteria can likely be explained by limited citrate production by CitZ.

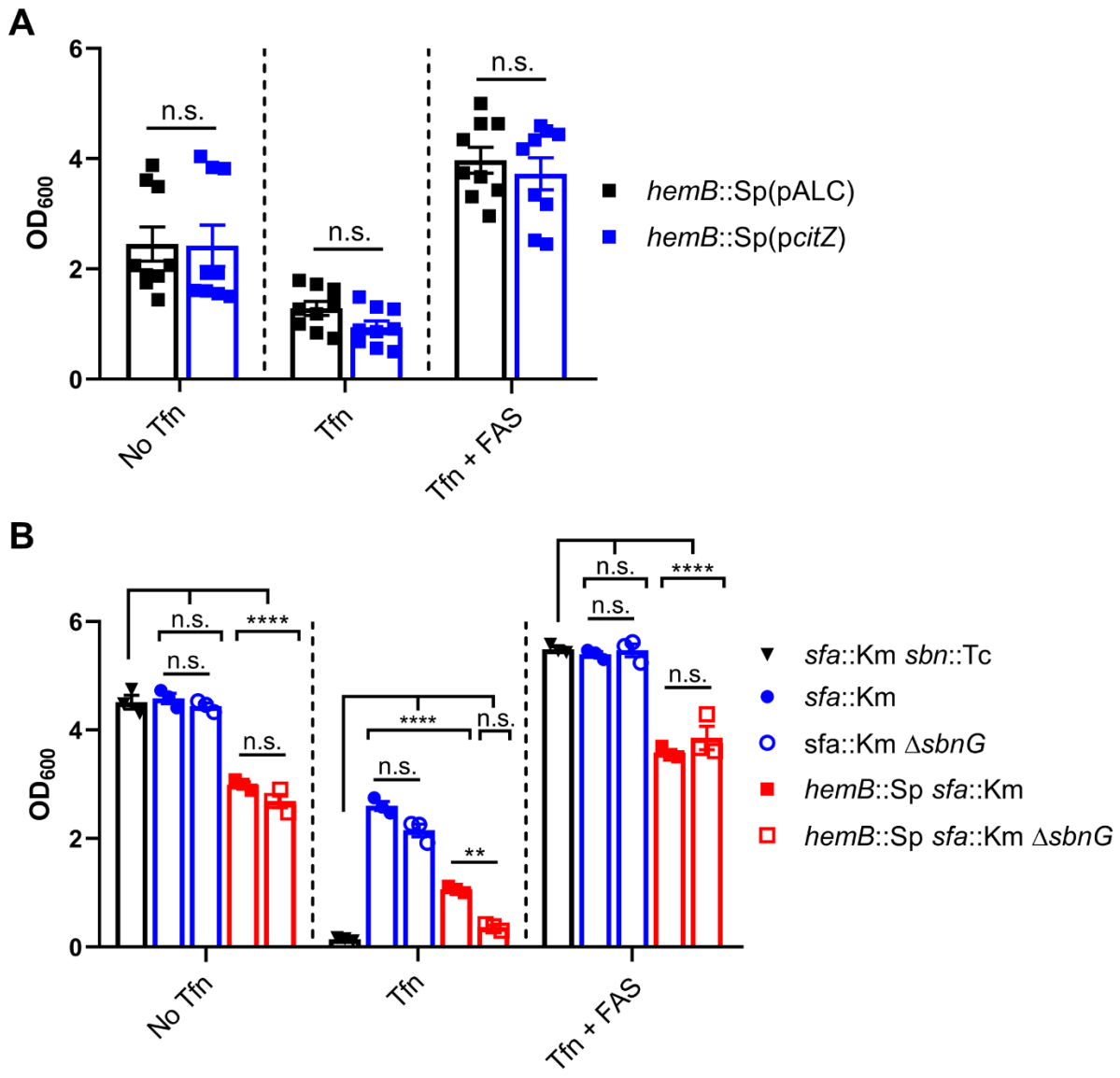

Figure 9. SB biosynthesis by *hemB*::Sp heavily relies on SbnG. (A-B) Growth in TMS supplemented with 0.4 µM hemin after 24 h. No Tfn, 5 µM Tfn, or 5 µM Tfn and 30 µM FAS was added to the media. Data are plotted as mean ± SEM, nine (A) or three (B) biological replicates. ** p<0.01, **** p<0.0001, one-way ANOVA with Tukey's post test.

3.7 *hemB*::Sp bacteria do not utilize staphyloferrin to support growth *in vivo*.

To determine whether *hemB*::Sp utilizes SA and/or SB *in vivo*, a murine model of systemic infection was used. Here, we infected mice with the *hemB*::Sp mutant, and siderophore biosynthesis mutants derived from the *hemB* SCV background. Compared to *hemB*::Sp bacteria, there was no significant difference in the percent weight loss or the bacterial loads in the kidneys and liver for the *hemB*::Sp staphyloferrin mutants at 48 h post-infection (Fig. 10A-C). These observations suggest that staphyloferrin is not required for growth by *hemB*::Sp bacteria *in vivo* despite the *hemB*::Sp *sbn*::Tc mutant demonstrating significant growth impairment *in vitro* when iron was restricted (Fig. 7A). Interestingly, the *hemB*::Sp *sbn*::Tc mutant had a significant increase in bacterial load in the liver of infected mice (Fig. 10C). However, it is unclear why higher bacterial counts were only observed in the livers of mice infected with the *hemB*::Sp *sbn*::Tc mutant. Growth of siderophore deficient *hemB S. aureus* was not attenuated *in vivo*, suggesting *hemB*::Sp bacteria do not require staphyloferrin biosynthesis to support growth *in vivo*.

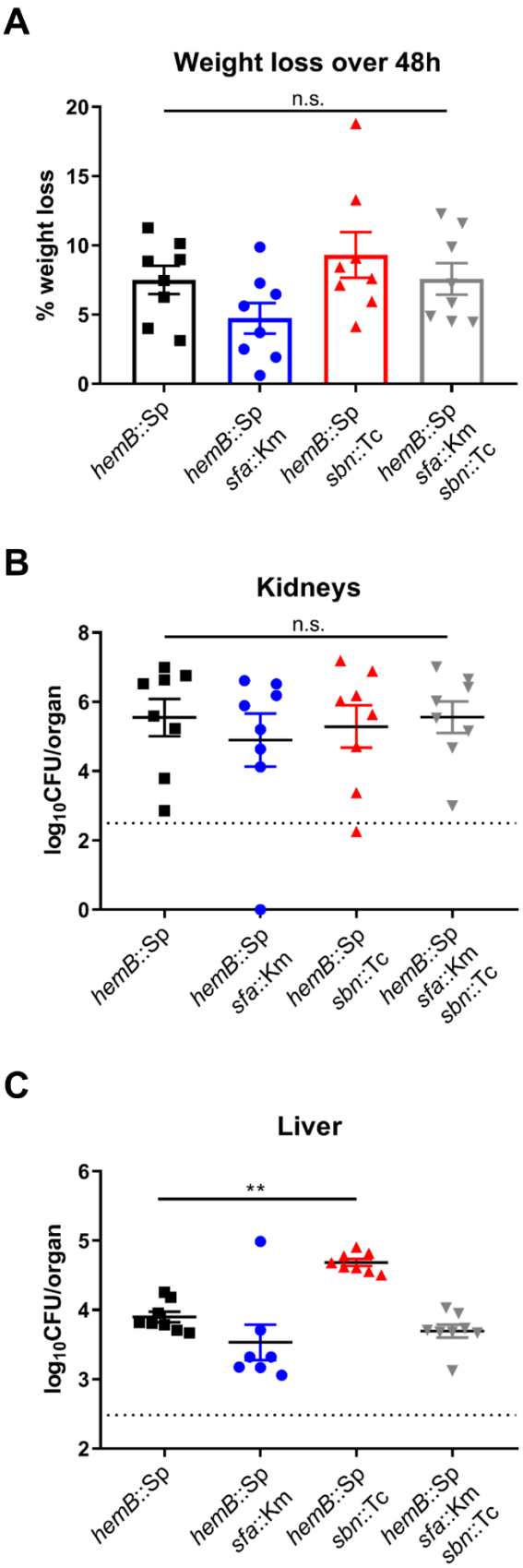
A
Weight loss over 48h
n.s.
% weight loss
20
15
10
5
0
hemB::Sp
hemB::Sp sfa::Km
hemB::Sp sbn::Tc
hemB::Sp sfa::Km sbn::Tc
B
Kidneys
n.s.
log10CFU/organ
8
6
4
2
0
hemB::Sp
hemB::Sp sfa::Km
hemB::Sp sbn::Tc
hemB::Sp sfa::Km sbn::Tc
C
Liver
**
log10CFU/organ
6
5
4
3
2
hemB::Sp
hemB::Sp sfa::Km
hemB::Sp sbn::Tc
hemB::Sp sfa::Km sbn::Tc

Figure 10. *hemB*::Sp bacteria do not utilize staphyloferrin to support growth *in vivo*. (A) Percent weight loss over 48 h of *S. aureus* SCV infected mice. **(B)** Bacterial burden in kidneys after 48 h**. (C)** Bacterial burden in liver after 48 h. Limit of accurate detection is indicated as a dashed line. Data are plotted as a mean ± SEM, at least seven animals per group. ** $p<0.01$, one-way ANOVA with Tukey's post test.

3.8 Hydroxamate-type siderophore utilization by *hemB*::Sp bacteria is dependent on hemin availability.

To investigate whether *hemB*::Sp bacteria utilize hydroxamate-type siderophores such as DFO, growth experiments with the previously described iron deplete and replete conditions were performed with DFO also added to media supplemented with Tfn. Growth of *S. aureus* in iron deplete and replete media mirrored prior results (Fig. 11A). Interestingly, the addition of DFO to *hemB*::Sp bacteria grown under iron restriction had no effect on growth (Fig. 11A). In contrast, DFO completely restored growth of the staphyloferrin deficient *S. aureus* mutant that was used as a control indicating DFO could function as a siderophore (Fig. 11A). Therefore, these observations indicated that *hemB*::Sp bacteria exhibit a defect in DFO utilization. Next, I considered whether these bacteria express $FhuD_2$, a component of the receptor required for hydroxamate-type siderophore (i.e. DFO) utilization. Whole cell lysates of *S. aureus* grown in media with excess iron or in the presence of Tfn were subject to Western blot analysis. A *fhuD*$_1$::Km *fhuD*$_2$::Tc mutant served as a negative control for expression of $FhuD_2$ (Fig. 11D). Importantly, WT, *hemB*::Sp, and *hemB*::Sp(p*hemB*) bacteria all expressed $FhuD_2$ in an iron-dependent manner when bacteria were grown in the presence of Tfn compared to media supplemented with excess iron (Fig. 11D). These data indicate that *hemB*::Sp bacteria likely still express the transport machinery for DFO uptake.

To examine whether DFO utilization by *hemB*::Sp bacteria was masked by SB utilization, I also examined DFO utilization by the *hemB*::Sp mutant deficient for staphyloferrin. A non-SCV staphyloferrin deficient mutant was used as the media control, to ensure iron restriction in the media and functionality of DFO (data not shown). As in previous experiments, the addition of Tfn eliminated growth of the *hemB*::Sp mutant with defective staphyloferrin biosynthesis and this growth defect was rescued by the addition of free iron in the form of FAS (Fig. 11B). Importantly, growth of the *hemB*:Sp *sfa*::Km *sbn*::Tc mutant was not recovered upon the addition of DFO to the iron-deplete media (Fig. 11B). In contrast, growth of the control *S. aureus* siderophore deficient

mutant fully recovered when growth media were supplemented with DFO as in Fig. 11A (data not shown). Therefore, *hemB*::Sp SCV bacteria appear to have a defect in DFO utilization.

To investigate whether the availability of hemin affects DFO utilization, a similar growth experiment with exogenously provided DFO was performed, but TMS was now supplemented with 2 µM hemin, a concentration previously found to increase growth rate, colony size, and pigmentation of *hemB*::Sp bacteria (see Fig. 3B and 11C). When additional hemin was added to the media, the *hemB*::Sp mutant grew to the same extent as WT bacteria in iron replete media, indicating that the additional hemin complemented the hemin auxotrophy, similar to complementation with p*hemB* (Fig. 11C). Surprisingly, when Tfn was added to TMS supplemented with 2 µM hemin, *hemB*::Sp bacteria still had a significant growth defect, as growth in iron deplete media was comparable to the *S. aureus* staphyloferrin deficient mutant (Fig. 11C). Thus, hemin supplementation may affect staphyloferrin utilization by *hemB*::Sp bacteria. However, provision of additional hemin enabled the utilization of DFO by the *hemB*::Sp mutant, as indicated by fully restored growth when the DFO was exogenously added to the media (Fig. 11C). Therefore, hydroxamate-type siderophore utilization by *hemB*::Sp bacteria is directly related to hemin availability.

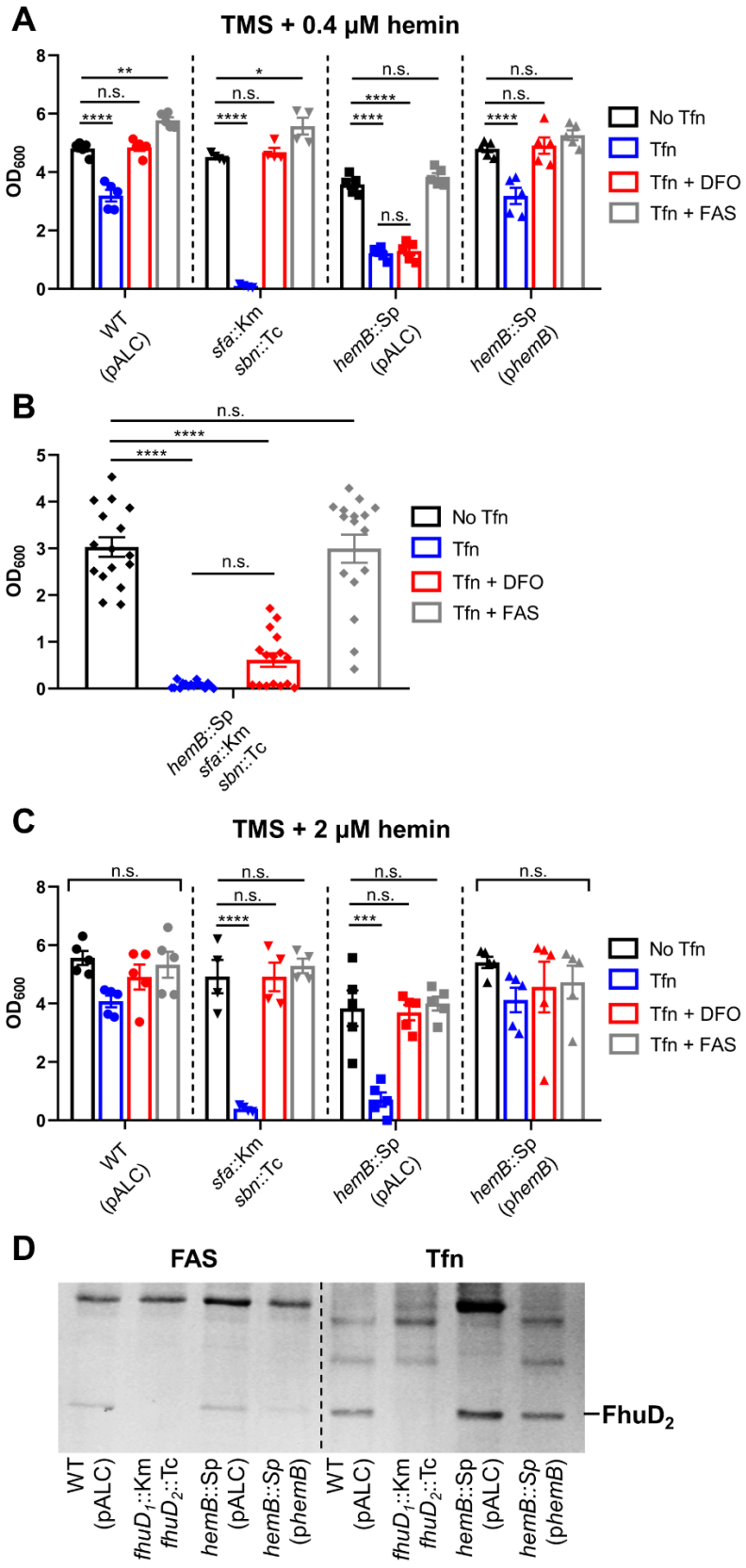
A
TMS + 0.4 μM hemin
OD600
No Tfn
Tfn
Tfn + DFO
Tfn + FAS
WT (pALC)
sfa::Km sbn::Tc
hemB::Sp (pALC)
hemB::Sp (phemB)
B
hemB::Sp sfa::Km sbn::Tc
C
TMS + 2 μM hemin
D
FAS
Tfn
FhuD2
WT (pALC)
fhuD1::Km fhuD2::Tc
hemB::Sp (pALC)
hemB::Sp (phemB)

Figure 11. DFO utilization by *hemB*::Sp is dependent on hemin availability. Growth in TMS supplemented with either **(A, B)** 0.4 µM hemin or **(C)** 2 µM hemin after 24 h. No Tfn, 5 µM Tfn, 5 µM Tfn and 30 µM FAS, or 5 µM Tfn and 100 µM DFO was added to the media. Data are plotted as mean ± SEM, at least four biological repeats (A,C) or sixteen biological repeats (6 individual experiments) (B). **** $p<0.0001$, one-way ANOVA with Tukey's post test. **(D)** Western blot for detection of $FhuD_2$ (34 kDa) in whole cell lysates prepared from cultures grown for 24 h in TMS supplemented with 0.4 µM hemin and either FAS (30 µM) or Tfn (1.5 µM).

3.9 Niche-specific utilization of DFO *in vivo* by *hemB*::Sp bacteria.

Previous work by the Heinrichs lab demonstrated that DFO augmented *S. aureus* USA300 virulence in a murine model of systemic infection[99]. To examine whether a *S. aureus hemB*::Sp mutant utilizes DFO *in vivo*, systemic infections were performed where mice were infected with WT and *hemB*::Sp bacteria. At the time of infection and at 24 h post-infection, 100 µL of DFO (10 mg/mL) or vehicle control was administered intraperitoneally. Infections were terminated at 48 h post-infection because WT infected mice that received DFO treatment met humane endpoint criteria at this timepoint. Compared to WT infected mice, *hemB*::Sp infected mice retained significantly more weight indicating that *hemB*::Sp bacteria were attenuated *in vivo* (Fig. 12A). Remarkably, administration of DFO only enhanced this effect and caused WT infected mice to lose significantly more weight as compared to WT infected animals without DFO and *hemB*::Sp infected animals with DFO (Fig. 12A). These observations indicated that *hemB*::Sp bacteria were attenuated *in vivo* and their pathogenic potential was not increased upon DFO administration.

At 48 h post-infection the bacterial burden in the hearts, kidneys, and livers of infected mice was also determined (Fig. 12B-D). In the hearts of infected animals, it was evident that the addition of DFO significantly enhanced the bacterial burden for WT bacteria but was without effect on *hemB*::Sp bacteria which only poorly colonized the heart (Fig. 12B). Furthermore, DFO treatment was without effect on the bacterial burden in the livers of *hemB*::Sp infected mice (Fig. 12B). In contrast, livers of WT infected mice had significantly increased bacterial burdens when animals received DFO (Fig. 12D). Remarkably, in the kidneys, DFO was used by WT and *hemB*::Sp bacteria in contrast to all other organs examined (Fig. 12C). Therefore, it is possible that there exists a niche-specific effect, where *hemB*::Sp bacteria have access a pool of hemin that enables DFO utilization in the kidneys. While these data demonstrated that DFO dramatically

increased virulence of WT bacteria *in vivo*, the same massive impact of DFO was not observed for *hemB*::Sp SCV bacteria. Therefore, it appears that *hemB*::Sp bacteria have a reduced ability to utilize DFO *in vivo*.

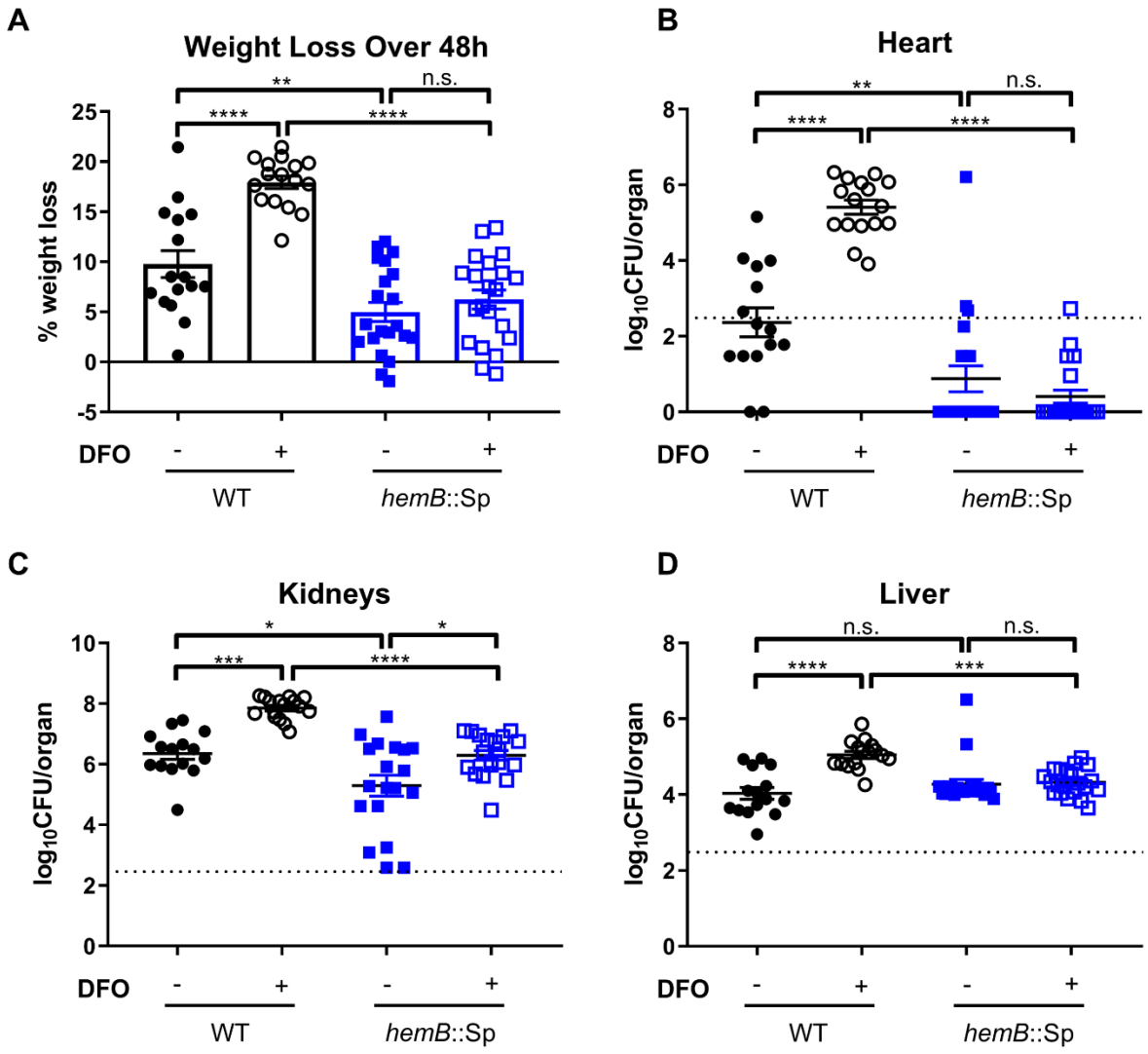

Figure 12. *In vivo* DFO utilization by WT and *hemB*::Sp bacteria. (A) Percent weight loss over 48 h of *S. aureus* SCV infected mice. **(B-D)** Bacterial burden in heart (B), kidneys (C), or liver (D) after 48 h. Limit of accurate detection is indicated as a dashed line. Data are plotted as a mean ± SEM, at least fifteen animals per group. * $p<0.05$, ** $p<0.01$, *** $p<0.001$, ****, $p<0.0001$, one-way ANOVA with Tukey's post test.

3.10 The *hemB*::Sp mutant has a defect in catechol-type siderophore utilization.

Stress hormones such as epinephrine have been shown to act as siderophores that support the growth of *S. aureus* in iron restricted environments[89]. To determine whether SCV bacteria can also utilize epinephrine, which is transported via the Sst siderophore uptake system, I examined whether epinephrine could promote growth of *S. aureus hemB*::Sp bacteria in the presence of Tfn. Growth of all the strains in the presence and absence of Tfn was comparable to previous experiments (Fig. 13). Importantly, epinephrine was found to be a functional siderophore because it recovered growth of the *S. aureus* staphyloferrin deficient mutant (Fig. 13). Remarkably, the addition of epinephrine to iron deplete media further inhibited growth of the *hemB*::Sp mutant (Fig. 13). Therefore, the addition of epinephrine negatively impacted growth of *hemB*::Sp bacteria. Furthermore, epinephrine did not rescue growth of the *hemB*::Sp mutant deficient for staphyloferrin biosynthesis (Fig. 13). Thus, epinephrine does not promote growth of *hemB*::Sp bacteria and utilization of catechol-type siderophores appears to be defective in *S. aureus* SCVs.

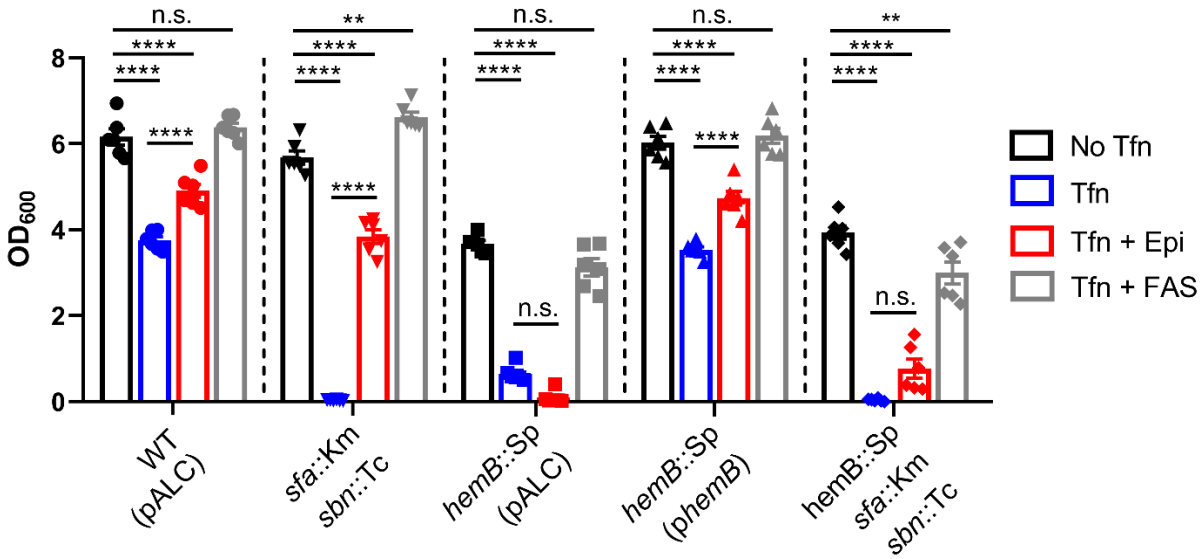

Figure 13. Epinephrine utilization by *hemB*::Sp. Growth in TMS supplemented with 0.4 µM hemin after 24 h. No Tfn, 5 µM Tfn, 5 µM Tfn and 30 µM FAS, or 5 µM Tfn and 100 µM epinephrine (Epi) was added to the media. Data are plotted as mean ± SEM, six biological replicates. **** p<0.0001, one-way ANOVA with Tukey's post test.

Chapter 4

4 Discussion and Future Directions

S. aureus is an opportunistic pathogen that colonizes roughly one third of the human population[2]. Alarmingly, *S. aureus* can display antibiotic resistance and cause severe, life-threatening infections in otherwise healthy individuals[12]. Consequently, *S. aureus* needs to acquire or synthesize essential nutrients within the host to proliferate during infection. Iron is one such nutrient but is unique as it is scarcely available, despite its abundance, due to its insolubility at biological pH and sequestration by the host, thereby preventing toxic effects of free iron and impeding growth of invading pathogens[42]. The iron acquisition strategies employed by WT *S. aureus* to overcome host sequestration of iron have been studied at length[33,63]. However, the mechanisms by which *S. aureus* SCVs acquire iron have not been explored despite the clinical relevance of SCVs. Therefore, this study aimed to gain insight into which *S. aureus* iron acquisition strategies are utilized by *S. aureus* SCVs.

Owing to the propensity of *S. aureus* SCVs isolated from clinical samples to revert to the WT phenotype, a genetically engineered stable SCV was generated. The *S. aureus hemB* mutant is an SCV that has been extensively described and implemented as a prototypic SCV for characterization of *S. aureus* SCVs because clinically isolated SCVs are often auxotrophic for hemin[103,113]. Therefore, a *hemB* mutant was used here to characterize the iron acquisition strategies of *S. aureus* SCVs. Consistent with the literature, mutation of *hemB* in the *S. aureus* USA300 background generated a stable SCV auxotrophic for hemin. Inactivation of *hemB* generates an SCV because *hemB* encodes the enzyme ALA dehydratase, which is essential for hemin biosynthesis in *S. aureus*[118]. The requirement for hemin biosynthesis is not unique to *S. aureus*, and other bacteria including Gram-negative organisms such as *E. coli* require hemin biosynthesis for optimal fitness[105,136]. Notably, *hemB* also encodes ALA dehydratase and catalyzes the same step of the hemin biosynthetic pathway in *E. coli*[137]. Moreover, inactivation of *hemB* in *E. coli* also results in an SCV phenotype due to the fact that hemin is an integral component of cytochromes in the ETC[105]. Consequently, hemin auxotrophs have deficient electron transport and a reduced capacity to synthesize ATP through oxidative phosphorylation[104]. Not surprisingly, *hemB* mutants are SCVs that display altered patterns of gene expression and the characteristic phenotypic switch to a slow growing bacterium that forms small colonies on solid media[104,113,121]. SCVs have also

been described for *P. aeruginosa*, a Gram-negative pathogen, and are associated with persistent lung infections in patients with CF, like *S. aureus* SCVs[138,139]. While the *hemB* gene of *P. aeruginosa* also encodes ALA dehydratase, and can complement an *E. coli hemB* mutant, a role for inactivation of *hemB* has not been attributed in *P. aeruginosa* SCV formation[140]. Instead, *P. aeruginosa* SCV formation has been associated with cyclic-di-GMP signalling pathways among other signaling systems[138]. Nevertheless, the *S. aureus hemB* mutant is as an archetypal SCV that has been used to characterize *S. aureus* SCVs.

Consistent with previous studies, the *S. aureus hemB*::Sp mutant could utilize exogenously provided hemin to overcome hemin auxotrophy. Provision of minimal hemin permitted reduced growth of SCV bacteria as compared to WT *S. aureus* in minimal medium, enabling the characterization of SCV iron acquisition mechanisms, and higher concentrations of hemin reverted growth of the *hemB*::Sp mutant to WT levels. Interestingly, utilization of hemin was independent of iron starvation, as hemin was utilized in iron replete medium. Expression of the Isd heme transport system is Fur dependent thus, active in iron-limited conditions[72]. Therefore, import of exogenous hemin is likely facilitated by an unidentified staphylococcal heme transport system independently of Fur regulation. Indeed, a study by Wright and Nair made use of a *hemB* mutant and determined that IsdE, the lipoprotein component of the Isd pathway, is dispensable for utilization of exogenously provided hemin[80]. Moreover, the role of HtsA in heme transport was investigated and also found dispensable for hemin utilization by a *hemB* mutant[80]. Since HtsABC is implicated in SA uptake, and specificity of HtsA for SA has been described, it is unlikely that the Hts transport system plays a role in heme transport, contrary to previous suggestion[71,81,82]. Thus, *S. aureus* must utilize at least one uncharacterized heme transport system. The *S. aureus* FepABC proteins, which bear homology to the *E. coli* EfeUOB system and are Fur-regulated, are under investigation for heme iron utilization[83,84]. EfeUOB-like systems are widespread in bacteria and have been implicated in iron utilization[83]. A study that cloned *fep* genes from *S. aureus* into an *E. coli* mutant lacking its own heme utilization systems determined that FepA and FepB enabled heme iron utilization[83]. However, the role of FepABC in *S. aureus* remains unknown and requires further examination. The study of heme iron utilization by *S. aureus* is complicated by expression of the Isd heme uptake system and by biosynthesis of heme. Therefore, I propose mutation of *fepABC* in the *hemB* mutant background lacking *isd* to characterize the role of these proteins in *S. aureus*. Furthermore, to elucidate the unidentified heme transport system that is uncoupled from

Fur regulation, I propose generation of a random transposon mutant library in the *hemB* mutant lacking *isd*, and identification of transposon mutants that have decreased heme utilization, as indicated by impeded reversion of the SCVs to the WT phenotype upon provision of exogenous hemin. Use of a *hemB* mutant to identify novel heme iron utilization mechanisms could enable a better understanding of the strategies employed by *S. aureus* to acquire heme iron, the preferred iron source of *S. aureus*, during infection[71].

In attempt to establish iron deplete conditions for the study of iron acquisition strategies employed by *S. aureus* SCVs using serum, I determined that FBS and HS should not be used in the characterization of *hemB* mutants. FBS was found to stimulate growth of *hemB*::Sp SCV bacteria to WT levels and therefore, *hemB* mutants are no longer SCVs in the presence of FBS. Importantly, FBS is routinely used to supplement cell culture media, despite being chemically undefined and poorly regulated[141]. In fact, studies that utilized a *hemB* mutant to characterize the intracellular survival of *S. aureus* SCVs in a variety of cell types supplemented their cell culture media with FBS[113,142,143]. While these studies reported differences among the WT strain and the isogenic *hemB* mutant, my work suggests that some skepticism should be applied when interpreting the results from studies that used FBS in their cell culture media. Indeed, recent work by the Heinrichs laboratory has demonstrated that extracellular content that is pinocytosed by macrophages is delivered to phagolysosomes, where phagocytosed *S. aureus* reside and begin to replicate[28,144]. Thus, it stands to reason that if FBS is added to cell culture media, hemin from the FBS would be delivered to the phagolysosome and would supplement the hemin auxotrophy of phagocytosed *S. aureus hemB* mutants, reverting the SCV phenotype. Future studies that aim to characterize intracellular survival or replication of *hemB* SCVs should therefore practice the use of serum free medium. In contrast, I found that HS impeded growth of the hemin auxotroph. While HS has previously been used to restrict iron in media, thereby impeding growth of the *S. aureus* staphyloferrin deficient mutant, the growth inhibition of *hemB*::Sp bacteria in the presence of HS was unrelated to iron availability[91,130]. It is possible that a contaminant of HS such as Hx, a heme binding serum protein that has been quantified from the sera of other animals, quenched the minimal hemin added that is required for growth of the *hemB*::Sp SCV[145]. Consequently, instead of using HS which contains Tfn, purified human apo-Tfn was used to chelate iron and establish an iron restricted condition, enabling the study of *S. aureus* SCV non-heme iron acquisition strategies.

Surprisingly, *hemB*::Sp bacteria were found to utilize SB, but not SA to support growth in iron deplete media, as indicated by abolished growth of SB biosynthetic and uptake mutants. In contrast, WT *S. aureus* utilizes both SA and SB when iron is limited, and it has been determined that mutation of SB biosynthesis or uptake results in growth delay, not growth abolishment, as SA compensates for the loss of SB. However, the *S. aureus hemB*::Sp mutant was found to use exogenously provided SA, indicating that defective SA utilization was due to aberrant SA biosynthesis rather than uptake. Indeed, the basis of deficient SA biosynthesis by *hemB*::Sp bacteria was found to be related to decreased availability of TCA cycle-derived citrate. It is known that *S. aureus* can only utilize TCA cycle-derived citrate for the biosynthesis of SA[92]. Thus, requirement of TCA cycle activity, specifically CitZ, the TCA cycle citrate synthase, for generation of SA has been established[92]. Moreover, it is known through studies of the transcriptional profile of *S. aureus* SCVs that TCA cycle activity is downregulated[120,121,128]. A transcriptome study of the *S. aureus hemB* mutant even reported downregulation of *citZ*[120]. However, a connection between decreased *citZ* expression in *S. aureus* SCVs and decreased biosynthesis of SA was never established. Therefore, my work provides evidence that the altered gene expression of SCVs impacts iron acquisition mechanisms utilized by the *S. aureus hemB*::Sp mutant. To support my findings, decreased TCA cycle activity of the *hemB*::Sp mutant could be confirmed by reverse transcription PCR (RT-PCR) of *citZ*.

The *in vitro* data presented here of siderophore utilization by *hemB*::Sp bacteria suggest that SB is salient for non-heme iron acquisition for *S. aureus* SCVs. Interestingly, SB has been speculated to be more important than SA for WT *S. aureus* virulence[33,92]. Since biosynthesis of SB is independent of TCA cycle activity, production of SB by WT *S. aureus* is unhindered by the paradoxical downregulation of TCA cycle genes by Fur in response to iron limitation, unlike SA[69,92]. Furthermore, all *S. aureus* genomes contain the SB biosynthetic locus, but it is rarely found among coagulase-negative staphylococci (CoNS), which represent a diverse group of staphylococcal species that are predominantly part of normal skin flora and are generally considered less pathogenic than *S. aureus*[87,146]. In contrast, the SA biosynthetic locus is conserved among CoNS and coagulase-positive staphylococci (CoPS)[81]. Taken together, this suggests that SB could provide an advantage over SA for WT *S. aureus* in the context of an infection. However, SB biosynthesis is regulated by SbnI, which binds heme and prevents SB production[134]. Consistent with this, the *hemB*::Sp mutant displayed a growth defect in iron deplete media supplemented with

additional hemin (Fig. 11C), presumably because of SbnI inhibition of SB biosynthesis. Therefore, the generation of SB by WT and SCV *S. aureus* could be downregulated *in vivo* where bacteria access sufficient quantities of heme. Moreover, a recent study by Perry *et al.* used matrix-assisted laser desorption/ionization Fourier transform ion cyclotron resonance imaging mass spectrometry (MALDI FT-ICR IMS) to characterize the distribution of SA and SB in heart, liver, and kidney abscesses formed during *S. aureus* infection[147]. Interestingly, the study found that the distribution of SA and SB was heterogenous – certain abscesses were more abundant in SB, no siderophore was detected in other foci, and surprisingly, SA was more prevalent than SB at most infection sites[147]. Therefore, it is more likely that SA and SB have niche-specific roles, and both contribute to *S. aureus* infection.

In the context of *S. aureus* SCV infections, it was hypothesized that SB utilization would be important because SA biosynthesis was impaired *in vitro*. Moreover, *S. aureus* SCVs have decreased toxin production, and therefore, may not access heme iron captured from lysed erythrocytes as efficiently as WT *S. aureus*[104]. Surprisingly, *hemB*::Sp mutants with impaired staphyloferrin biosynthesis were not attenuated in the murine model of systemic infection. Thus, SA and SB do not contribute to the fitness of *S. aureus hemB*::Sp bacteria *in vivo*. In fact, the *hemB*::Sp mutant with disrupted SB biosynthesis, which was severely impaired *in vitro*, may have increased fitness in the liver of infected mice, as indicated by the greater number of bacteria recovered. To determine whether impaired SB utilization does indeed improve fitness of the *hemB*::Sp mutant, this experiment should be repeated with the *hemB*::Sp *sirA*::Km mutant, which has disrupted SB uptake. Notably, WT *S. aureus* staphyloferrin biosynthetic mutants are similarly not attenuated in a murine model of systemic infection, except in the heart, highlighting that *in vivo* iron acquisition by *S. aureus* is complex and involves several factors including SA and SB[89]. Indeed, the combination of impaired SA, SB, and catechol-type siderophore uptake was required for decreased bacterial burdens in the liver and kidneys of *S. aureus* infected mice[89]. However, unlike WT *S. aureus*, the *hemB*::Sp mutant did not use epinephrine, a catechol-type siderophore, *in vitro*. In fact, growth of the *hemB*::Sp mutant was decreased in iron deplete media upon provision of epinephrine, indicating epinephrine impedes SB utilization by competing with SB for Tfn-Fe^{3+}. Thus, a role for catechol-type siderophore uptake for *S. aureus* SCVs *in vivo* is unlikely. Consequently, I propose that heme iron acquisition is critical for *S. aureus* SCVs during systemic infection. As mentioned, Isd remains the only well-characterized *S. aureus* heme acquisition

system. My work suggests that an emphasis should be placed on elucidating alternative heme transport mechanisms to understand how WT *S. aureus* and *S. aureus* SCVs acquire heme *in vivo*. Moreover, MALDI FT-ICR IMS could be used to identify the presence of staphyloferrin in abscesses formed during infection with the *S. aureus hemB*::Sp mutant before dismissing *in vivo* staphyloferrin utilization by SCVs.

To investigate hydroxamate-type siderophore utilization by *S. aureus* SCVs, growth promotion by DFO, a clinically relevant iron chelator used to treat iron overload, was examined. It was previously shown that DFO is utilized by *S. aureus* and that DFO exacerbates *S. aureus* virulence in a murine model of systemic infection[61,88,99]. Consistent with this, WT *S. aureus* infected mice that were treated with DFO in this study lost substantially more weight, and the bacterial burdens recovered from the heart, kidneys, and liver were higher. In contrast, the *hemB*::Sp mutant had defective DFO utilization *in vitro* and *in vivo*. However, DFO could be utilized by *S. aureus hemB*::Sp bacteria upon provision of additional hemin *in vitro*. Furthermore, a niche-specific increase in the bacterial burden upon DFO treatment was found in the kidneys of *hemB*::Sp infected mice. Therefore, I speculate that the *hemB*::Sp mutant acquires heme in the kidneys upon tissue damage which enables DFO utilization. The heme-dependent use of DFO by the *hemB*::Sp mutant in the kidneys was unexpected given the focus on *S. aureus* SCV intracellular persistence due to decreased expression of toxins, such as α-toxin, in the literature[104]. Thus, *in vivo* heme utilization and toxin production by the *hemB*::Sp mutant should be investigated. For this, *isd* and *hla* (α-toxin) mutants could be generated in the *hemB*::Sp background and used to infect mice to determine whether the Isd system and/or α-toxin contribute to *S. aureus* SCV pathogenicity. Moreover, if any additional heme acquisition systems are identified, they should also be examined in the context of *S. aureus* SCVs.

Notably, the virulence of the *S. aureus* SCVs has been studied with various animal models, and it has been suggested that the *hemB* mutant is less virulent than WT *S. aureus*. Indeed, a *hemB* mutant was attenuated relative to WT *S. aureus* in a murine model of osteomyelitis[119]. In a murine model of septic arthritis, mice infected with the *hemB* mutant demonstrated more severe arthritis, purportedly due to increased protease production, but had lower bacterial burden in their kidneys and joints than mice infected with WT *S. aureus*[148]. Furthermore, in a murine mastitis model, the *hemB* mutant had reduced capacity to colonize the mammary glands[149]. In a rabbit endocarditis model, however, bacterial burden of the *hemB* mutant and WT *S. aureus* in the kidneys and spleen

were not significantly different[114]. It was theorized that bacterial burdens were similar because of increased hemin availability in organs due to tissue damage in the endocarditis model, enabling restoration of the WT phenotype[114]. Consistent with the notion that *S. aureus* SCVs are attenuated relative to WT *S. aureus*, the data presented here demonstrated that mice infected with the *hemB*::Sp mutant lost significantly less weight than WT *S. aureus* infected mice. Moreover, the *hemB*::Sp mutant colonized the heart poorly compared to WT *S. aureus*, and the bacterial burden in the kidneys of *hemB*::Sp infected mice was lower than that of mice infected with WT *S. aureus*. This is indicative of decreased clonal expansion and spread to other organs by SCV bacteria following initial capture by the Kupffer cells – the resident liver macrophages – in a systemic infection, presumably due to slow growth[148,150]. Notably, since *S. aureus hemB*::Sp bacteria were recovered from the kidneys, this stipulates that the *hemB*::Sp mutant replicates *in vivo* and must acquire iron to do so. Interestingly, the bacterial load in the liver was comparable for mice infected with the *hemB*::Sp mutant and mice infected with WT *S. aureus*. It is possible that *hemB*::Sp bacteria are captured by Kupffer cells equally as well as WT *S. aureus* and withstand the host immune response to prevent clearing and persist within the liver. Thus, future research should investigate the intracellular persistence and replication of *S. aureus* SCVs within macrophages, as well as the infection dynamics of *S. aureus* SCVs. A better understanding of the niches occupied by *S. aureus* SCVs and the progression of infections they cause is necessary to inform the development of novel therapeutics specific for treatment of *S. aureus* SCV infections.

In my investigation of iron acquisition strategies of *S. aureus* SCVS, I identified that xenosiderophore utilization was defective in the *hemB*::Sp mutant, however, the reason remains unknown. Fur regulated expression of iron regulated genes such as HtsA, SirA, and $FhuD_2$, the receptors for SB, SA, and hydroxamate-type siderophores, respectively, was found to be normal. Therefore, it is unlikely that SstD, the receptor for catechol-type siderophores, or other iron regulated genes are differentially expressed in the *hemB*::Sp mutant, unless subject to secondary regulation as in the case of SbnI regulation of SB biosynthetic genes. I hypothesize that defective siderophore utilization is related to decreased energy for siderophore uptake and/or decreased ability to extract iron from intracellular siderophore. Siderophore uptake is an energy dependent process powered by ATP hydrolysis. The FhuC ATPase is required for SA, SB, and hydroxamate-type siderophore uptake, while SstC is the ATPase involved in catechol-type siderophore uptake[81,98,101]. *S. aureus* SCVs have decreased ATP levels due to aberrant ETC activity[104,113].

Therefore, it stands to reason that siderophore uptake may be negatively impacted. Consistent with this notion, there appeared to be a limit on staphyloferrin utilization by the *hemB*::Sp mutant, indicated by a "maximal" level of growth that could be achieved through SB or SA utilization in iron deplete media (Fig. 8B). To examine whether ATP levels in the *hemB*::Sp mutant affect xenosiderophore utilization, media supplemented with hexose phosphates and other carbohydrates, which enable ATP generation independently of the ETC, could be used to investigate DFO and epinephrine utilization by *S. aureus hemB*::Sp bacteria[122]. To confirm that any differences in siderophore utilization are due to differences in intracellular ATP levels, an ATP detection kit could be used to measure intracellular ATP levels of the *hemB*::Sp mutant with and without provision of additional carbon sources. Even if *S. aureus* SCVs successfully uptake siderophore, iron must be freed from the siderophore before it can be utilized. To free iron from siderophores, bacteria express enzymes that degrade siderophores or reductases that reduce Fe^{3+} to Fe^{2+}, which has a lower affinity for siderophores[130]. Although the process of iron extraction from siderophores is still poorly understood for *S. aureus*, iron utilization oxidoreductase (IruO) is implicated in iron acquisition from Fe-DFO and NtrA, a nitroreductase, is required for iron utilization from Fe-SA[130]. I speculate that *S. aureus* SCVs, which have altered metabolism, may have decreased levels of nicotinamide adenine dinucleotide phosphate (NADPH), which is required for the activity of reductases, potentially limiting iron extraction from siderophores[151–153]. Therefore, the intracellular levels of NADPH in the *hemB*::Sp mutant should be examined by use of a NADPH detection kit. Esterases have been described in other bacterial species for the breakdown of catechol-type siderophores, but it is unknown how *S. aureus* frees iron from catechol-type siderophores[130,154,155]. A better understanding of the strategies *S. aureus* utilizes for iron extraction from catechol-type siderophores is required to determine whether the defective utilization of epinephrine by *S. aureus* SCVs was related to extraction of iron from the siderophore. In summary, metabolic and energetic differences of *S. aureus* SCVs could limit their ability to uptake siderophore and extract non-heme iron for utilization.

While this study focused on the *S. aureus hemB*::Sp mutant, future investigations should examine the iron acquisition strategies employed by other SCVs, such as a menadione auxotroph. Notably, mutations in genes part of the *men* operon have been identified in several *S. aureus* SCV clinical isolates and the *S. aureus menD* mutant, similar to the *hemB* mutant, has also been extensively described[104,115,116]. The *menD* gene encodes an enzyme involved in the biosynthesis of

menaquinone, a component of the ETC, thus mutation of *menD* results in defective oxidative phosphorylation, as with the *hemB* mutant[104]. I hypothesize a *S. aureus menD* mutant will also have a defect in SA biosynthesis, due to downregulated TCA cycle activity[156]. Therefore, I propose that the iron acquisition strategies employed by a *S. aureus* Δ*menD* mutant should be compared to those of the *hemB*::Sp mutant, by repeating the same experiments performed here. Furthermore, the iron acquisition strategies of SCVs from another staphylococcal species, such as *Staphylococcus epidermidis* could be examined. *S. epidermidis* is a CoNS and a notable cause of nosocomial infections[146]. *S. epidermidis* SCVs are often isolated from prosthetic joint infections, thus, must acquire iron to persist in the host[157,158]. Interestingly, the genome of *S. epidermidis* does not contain the *sbn* operon, required for SB biosynthesis[87]. Consequently, growth of *S. epidermidis* in iron deplete media is dependent on SA utilization. Therefore, if *S. epidermidis* SCVs also have a defect in SA biosynthesis, no growth will be observed in iron deplete media. The study of iron acquisition mechanisms important for other *S. aureus* SCVs and other staphylococcal SCVs will allow the identification and generalization of the iron acquisition strategies important for SCVs.

The work presented here provides valuable insight into how the *hemB*::Sp mutant, a *S. aureus* SCV acquires iron (summarized in Table 3). While *S. aureus* iron acquisition strategies have been studied at length, little was known about how *S. aureus* SCVs acquire iron. Notably, *hemB*::Sp bacteria sustained growth in iron deplete media due to utilization of SB, but not SA. Downregulated TCA cycle activity of *S. aureus* SCVs was determined to disrupt SA biosynthesis, but *S. aureus hemB*::Sp bacteria could utilize exogenously provided SA. *In vivo*, SA and SB did not contribute to infectivity of *hemB*::Sp bacteria. Moreover, utilization of DFO and epinephrine, hydroxamate-type and catechol-type siderophores, respectively, by *hemB*::Sp bacteria was defective in iron deplete media. Furthermore, DFO did not augment virulence of the *hemB*::Sp mutant in a murine model of systemic infection. Importantly, my work uncovered the impact of energetic limitations, metabolic changes, and altered gene expression associated with SCV bacteria on iron acquisition strategies employed by *S. aureus* SCVs. Due to the fact that iron is essential for bacterial growth, and *S. aureus* SCVs cause persistent infections that are difficult to treat, insights into the iron acquisition strategies employed by *S. aureus* SCVs are critical for understanding these pathogens, and for the potential identification of novel drug targets that if perturbed, could inhibit *S. aureus* SCV infection.

Table 3. Summary of iron acquisition strategies employed by *S. aureus* SCVs.

	WT		***hemB*::Sp**	
Iron Source	**Synthesize**	**Utilize**	**Synthesize**	**Utilize**
Heme	+	+	-	+
SA	+	+	-	+
SB	+	+	+	+
DFO	N/A	+	N/A	-
Epinephrine	N/A	+	N/A	-

References

1. Williams, R. E. Healthy carriage of *Staphylococcus aureus*: its prevalence and importance. *Bacteriol. Rev.* **27**, 56–71 (1963).
2. Wertheim, H. F. L. *et al.* The role of nasal carriage in *Staphylococcus aureus* infections. *Lancet Infect. Dis.* **5**, 751–762 (2005).
3. Williams, R. E. *et al.* Nasal staphylococci and sepsis in hospital patients. *Br. Med. J.* **2**, 658–62 (1959).
4. Davis, K. A., Stewart, J. J., Crouch, H. K., Florez, C. E. & Hospenthal, D. R. Methicillin-resistant *Staphylococcus aureus* (MRSA) nares colonization at hospital admission and its effect on subsequent MRSA infection. *Clin. Infect. Dis.* **39**, 776–82 (2004).
5. Kluytmans, J., van Belkum, A. & Verbrugh, H. Nasal carriage of *Staphylococcus aureus*: epidemiology, underlying mechanisms, and associated risks. *Clin. Microbiol. Rev.* **10**, 505–20 (1997).
6. Klevens, R. M. *et al.* Invasive methicillin-resistant *Staphylococcus aureus* infections in the United States. *JAMA* **298**, 1763–71 (2007).
7. Moran, G. J. *et al.* Methicillin-resistant *S. aureus* infections among patients in the emergency department. *N. Engl. J. Med.* **355**, 666–74 (2006).
8. Boucher, H., Miller, L. G. & Razonable, R. R. Serious infections caused by methicillin-resistant *Staphylococcus aureus*. *Clin. Infect. Dis.* **51**, S183–S197 (2010).
9. Kirby, W. M. Extraction of a highly potent penicillin inactivator from penicillin resistant staphylococci. *Science* **99**, 452–3 (1944).
10. Jevons, M. P. 'Celbenin'-resistant staphylococci. *Br. Med. J.* **1**, 124–125 (1961).
11. Barber, M. Methicillin-resistant staphylococci. *J. Clin. Pathol.* **14**, 385–93 (1961).
12. Lakhundi, S. & Zhang, K. Methicillin-resistant *Staphylococcus aureus*: molecular characterization, evolution, and epidemiology. *Clin. Microbiol. Rev.* **31**, 1–103 (2018).
13. Fridkin, S. K. *et al.* Methicillin-resistant *Staphylococcus aureus* disease in three communities. *N. Engl. J. Med.* **352**, 1436–44 (2005).
14. Miller, L. G. *et al.* Necrotizing fasciitis caused by community-associated methicillin-resistant *Staphylococcus aureus* in Los Angeles. *N. Engl. J. Med.* **352**, 1445–53 (2005).
15. King, M. D. *et al.* Emergence of community-acquired methicillin-resistant *Staphylococcus aureus* USA 300 clone as the predominant cause of skin and soft-tissue infections. *Ann.*

Intern. Med. **144**, 309–17 (2006).

16. Tenover, F. C. *et al.* Characterization of *Staphylococcus aureus* isolates from nasal cultures collected from individuals in the United States in 2001 to 2004. *J. Clin. Microbiol.* **46**, 2837–41 (2008).
17. Bien, J., Sokolova, O. & Bozko, P. Characterization of virulence factors of *Staphylococcus aureus*: novel function of known virulence factors that are implicated in activation of airway epithelial proinflammatory response. *J. Pathog.* **2011**, 601905 (2011).
18. Flannagan, R. S., Heit, B. & Heinrichs, D. E. Antimicrobial mechanisms of macrophages and the immune evasion strategies of *Staphylococcus aureus*. *Pathogens* **4**, 826–68 (2015).
19. Thammavongsa, V., Kim, H. K., Missiakas, D. & Schneewind, O. Staphylococcal manipulation of host immune responses. *Nat. Rev. Microbiol.* **13**, 529–43 (2015).
20. Foster, T. J., Geoghegan, J. A., Ganesh, V. K. & Höök, M. Adhesion, invasion and evasion: the many functions of the surface proteins of *Staphylococcus aureus*. *Nat. Rev. Microbiol.* **12**, 49–62 (2014).
21. Foster, T. J. Immune evasion by staphylococci. *Nat. Rev. Microbiol.* **3**, 948–58 (2005).
22. Spaan, A. N., Surewaard, B. G. J., Nijland, R. & van Strijp, J. A. G. Neutrophils versus *Staphylococcus aureus* : a biological tug of war. *Annu. Rev. Microbiol.* **67**, 629–650 (2013).
23. Ko, Y. P. *et al.* Phagocytosis escape by a *Staphylococcus aureus* protein that connects complement and coagulation proteins at the bacterial surface. *PLoS Pathog.* **9**, 1–13 (2013).
24. Peterson, P. K., Verhoef, J. A. N., Sabath, L. D. & Quie, P. G. Effect of protein A on staphylococcal opsonization. **15**, 760–764 (1977).
25. Gresham, H. D. *et al.* Survival of *Staphylococcus aureus* inside neutrophils contributes to infection. *J. Immunol.* **164**, 3713–3722 (2000).
26. Hamza, T. & Li, B. Differential responses of osteoblasts and macrophages upon *Staphylococcus aureus* infection. *BMC Microbiol.* **14**, 207 (2014).
27. Kubica, M. *et al.* A potential new pathway for *Staphylococcus aureus* dissemination: the silent survival of *S. aureus* phagocytosed by human monocyte-derived macrophages. *PLoS One* **3**, e1409 (2008).
28. Flannagan, R. S., Heit, B. & Heinrichs, D. E. Intracellular replication of *Staphylococcus aureus* in mature phagolysosomes in macrophages precedes host cell death, and bacterial escape and dissemination. *Cell. Microbiol.* **18**, 514–35 (2016).

29. Alonzo, F. & Torres, V. J. The bicomponent pore-forming leucocidins of *Staphylococcus aureus*. *Microbiol. Mol. Biol. Rev.* **78**, 199–230 (2014).
30. Berube, B. J. & Wardenburg, J. B. *Staphylococcus aureus* α-toxin: Nearly a century of intrigue. *Toxins (Basel).* **5**, 1140–1166 (2013).
31. Peschel, A. & Otto, M. Phenol-soluble modulins and staphylococcal infection. *Nat. Rev. Microbiol.* **11**, 667–73 (2013).
32. Kaiser, J. C. & Heinrichs, D. E. Branching out: alterations in bacterial physiology and virulence due to branched-chain amino acid deprivation. *MBio* **9**, 1–17 (2018).
33. Sheldon, J. R. & Heinrichs, D. E. Recent developments in understanding the iron acquisition strategies of gram positive pathogens. *FEMS Microbiol. Rev.* **39**, 592–630 (2015).
34. Posey, J. E. & Gherardini, F. C. Lack of a role for iron in the Lyme disease pathogen. *Science* **288**, 1651–3 (2000).
35. Weinberg, E. D. The *Lactobacillus* anomaly: total iron abstinence. *Perspect. Biol. Med.* **40**, 578–83 (1997).
36. Hood, M. I. & Skaar, E. P. Nutritional immunity: transition metals at the pathogen–host interface. *Nat. Rev. Microbiol.* **10**, 525–537 (2012).
37. Fenton, H. J. H. LXXIII.—Oxidation of tartaric acid in presence of iron. *J. Chem. Soc., Trans.* **65**, 899–910 (1894).
38. Haber, F. & Weiss, J. Über die katalyse des hydroperoxydes. *Naturwissenschaften* **20**, 948–950 (1932).
39. Ezraty, B., Gennaris, A., Barras, F. & Collet, J.-F. Oxidative stress, protein damage and repair in bacteria. *Nat. Rev. Microbiol.* **15**, 385–396 (2017).
40. Imlay, J. A. & Linn, S. DNA damage and oxygen radical toxicity. *Science* **240**, 1302–1309 (1988).
41. Wienk, K. J. H., Marx, J. J. M. & Beynen, A. C. The concept of iron bioavailability and its assessment. *Eur. J. Nutr.* **38**, 51–75 (1999).
42. Ratledge, C. & Dover, L. G. Iron metabolism in pathogenic bacteria. *Annu. Rev. Microbiol.* **54**, 881–941 (2000).
43. Chipperfield, J. R. & Ratledge, C. Salicylic acid is not a bacterial siderophore: a theoretical study. *Biometals* **13**, 165–8 (2000).
44. Hennigar, S. R. & McClung, J. P. Nutritional immunity: starving pathogens of trace

minerals. *Am. J. Lifestyle Med.* **10**, 170–173 (2014).

45. Cassat, J. E. & Skaar, E. P. Iron in infection and immunity. *Cell Host Microbe* **13**, 509–519 (2013).
46. Fuqua, B. K., Vulpe, C. D. & Anderson, G. J. Intestinal iron absorption. *J. Trace Elem. Med. Biol.* **26**, 115–119 (2012).
47. Przybyszewska, J. & Zekanowska, E. The role of hepcidin, ferroportin, HCP1, and DMT1 protein in iron absorption in the human digestive tract. *Prz. Gastroenterol.* **9**, 208–213 (2014).
48. Anderson, G. J. & Frazer, D. M. Current understanding of iron homeostasis. *Am. J. Clin. Nutr.* **106**, 1559S-1566S (2017).
49. Le Blanc, S., Garrick, M. D. & Arredondo, M. Heme carrier protein 1 transports heme and is involved in heme-Fe metabolism. *Am. J. Physiol.* **302**, C1780-5 (2012).
50. Gunshin, H. *et al.* Cloning and characterization of a mammalian proton-coupled metal-ion transporter. *Nature* **388**, 482–8 (1997).
51. McKie, A. T. *et al.* An iron-regulated ferric reductase associated with the absorption of dietary iron. *Science* **291**, 1755–9 (2001).
52. Donovan, A. *et al.* The iron exporter ferroportin/Slc40a1 is essential for iron homeostasis. *Cell Metab.* **1**, 191–200 (2005).
53. Lane, D. J. R. *et al.* Cellular iron uptake, trafficking and metabolism: Key molecules and mechanisms and their roles in disease. *Biochim. Biophys. Acta* **1853**, 1130–44 (2015).
54. Sendamarai, A. K., Ohgami, R. S., Fleming, M. D. & Lawrence, C. M. Structure of the membrane proximal oxidoreductase domain of human Steap3, the dominant ferrireductase of the erythroid transferrin cycle. *Proc. Natl. Acad. Sci. U. S. A.* **105**, 7410–7415 (2008).
55. Johnson-Wimbley, T. D. & Graham, D. Y. Diagnosis and management of iron deficiency anemia in the 21st century. *Therap. Adv. Gastroenterol.* **4**, 177–84 (2011).
56. McLean, E., Cogswell, M., Egli, I., Wojdyla, D. & de Benoist, B. Worldwide prevalence of anaemia, WHO Vitamin and Mineral Nutrition Information System, 1993-2005. *Public Health Nutr.* **12**, 444–54 (2009).
57. Geller, S. A. & de Campos, F. P. F. Hereditary hemochromatosis. *Autops. case reports* **5**, 7–10 (2015).
58. Gerhard, G. S., Paynton, B. V. & DiStefano, J. K. Identification of genes for hereditary

hemochromatosis. in *Methods in Molecular Biology* 353–365 (2018).

59. Vujić, M. Molecular basis of HFE-hemochromatosis. *Front. Pharmacol.* **5**, 42 (2014).
60. Mobarra, N. *et al.* A review on iron chelators in treatment of iron overload syndromes. *Int. J. Hematol. stem cell Res.* **10**, 239–247 (2016).
61. Sebulsky, M. T., Hohnstein, D., Hunter, M. D. & Heinrichs, D. E. Identification and characterization of a membrane permease involved in iron-hydroxamate transport in *Staphylococcus aureus*. *J. Bacteriol.* **182**, 4394–400 (2000).
62. Brock, J. H. & Ng, J. The effect of desferrioxamine on the growth of *Staphylococcus aureus*, *Yersinia enterocolitica* and *Streptococcus faecalis* in human serum: Uptake of desferrioxamine-bound iron. *FEMS Microbiol. Lett.* **20**, 439–442 (1983).
63. Hammer, N. D. & Skaar, E. P. The impact of metal sequestration on *Staphylococcus aureus* metabolism. *Curr. Opin. Microbiol.* **15**, 10–4 (2012).
64. Xiong, A., Singh, V. K., Cabrera, G. & Jayaswal, R. K. Molecular characterization of the ferric-uptake regulator, fur, from *Staphylococcus aureus*. *Microbiology* **146**, 659–668 (2000).
65. Horsburgh, M. J., Ingham, E. & Foster, S. J. In *Staphylococcus aureus*, Fur is an interactive regulator with PerR, contributes to virulence, and is necessary for oxidative stress resistance through positive regulation of catalase and iron homeostasis. *J. Bacteriol.* **183**, 468–475 (2001).
66. Torres, V. J. *et al. Staphylococcus aureus fur* regulates the expression of virulence factors that contribute to the pathogenesis of pneumonia. *Infect. Immun.* **78**, 1618–28 (2010).
67. Reniere, M. L. & Skaar, E. P. *Staphylococcus aureus* haem oxygenases are differentially regulated by iron and haem. *Mol. Microbiol.* **69**, 1304–15 (2008).
68. Pishchany, G., Dickey, S. E. & Skaar, E. P. Subcellular localization of the *Staphylococcus aureus* heme iron transport components IsdA and IsdB. *Infect. Immun.* **77**, 2624–34 (2009).
69. Friedman, D. B. *et al. Staphylococcus aureus* redirects central metabolism to increase iron availability. *PLoS Pathog.* **2**, 0777–0789 (2006).
70. Johnson, M., Cockayne, A., Williams, P. H. & Morrissey, J. a. Iron-responsive regulation of biofilm formation in *Staphylococcus aureus* involves *fur*-dependent and *fur*-independent mechanisms. *J. Bacteriol.* **187**, 8211–5 (2005).
71. Skaar, E. P., Humayun, M., Bae, T., DeBord, K. L. & Schneewind, O. Iron-source

preference of *Staphylococcus aureus* infections. *Science* **305**, 1626–8 (2004).

72. Mazmanian, S. K. *et al.* Passage of heme-iron across the envelope of *Staphylococcus aureus*. *Science* **299**, 906–9 (2003).
73. Mazmanian, S. K., Ton-That, H., Su, K. & Schneewind, O. An iron-regulated sortase anchors a class of surface protein during *Staphylococcus aureus* pathogenesis. *Proc. Natl. Acad. Sci. U. S. A.* **99**, 2293–8 (2002).
74. Dryla, A., Gelbmann, D., von Gabain, A. & Nagy, E. Identification of a novel iron regulated staphylococcal surface protein with haptoglobin-haemoglobin binding activity. *Mol. Microbiol.* **49**, 37–53 (2003).
75. Torres, V. J., Pishchany, G., Humayun, M., Schneewind, O. & Skaar, E. P. *Staphylococcus aureus* IsdB is a hemoglobin receptor required for heme iron utilization. *J. Bacteriol.* **188**, 8421–9 (2006).
76. Liu, M. *et al.* Direct hemin transfer from IsdA to IsdC in the iron-regulated surface determinant (Isd) heme acquisition system of *Staphylococcus aureus*. *J. Biol. Chem.* **283**, 6668–76 (2008).
77. Muryoi, N. *et al.* Demonstration of the iron-regulated surface determinant (Isd) heme transfer pathway in *Staphylococcus aureus*. *J. Biol. Chem.* **283**, 28125–36 (2008).
78. Grigg, J. C., Vermeiren, C. L., Heinrichs, D. E. & Murphy, M. E. P. Heme coordination by *Staphylococcus aureus* IsdE. *J. Biol. Chem.* **282**, 28815–22 (2007).
79. Skaar, E. P., Gaspar, A. H. & Schneewind, O. IsdG and IsdI, heme-degrading enzymes in the cytoplasm of *Staphylococcus aureus*. *J. Biol. Chem.* **279**, 436–43 (2004).
80. Wright, J. A. & Nair, S. P. The lipoprotein components of the Isd and Hts transport systems are dispensable for acquisition of heme by *Staphylococcus aureus*. *FEMS Microbiol. Lett.* **329**, 177–85 (2012).
81. Beasley, F. C. *et al.* Characterization of staphyloferrin A biosynthetic and transport mutants in *Staphylococcus aureus*. *Mol. Microbiol.* **72**, 947–63 (2009).
82. Grigg, J. C., Cooper, J. D., Cheung, J., Heinrichs, D. E. & Murphy, M. E. P. The *Staphylococcus aureus* siderophore receptor HtsA undergoes localized conformational changes to enclose staphyloferrin A in an arginine-rich binding pocket. *J. Biol. Chem.* **285**, 11162–71 (2010).
83. Turlin, E., Débarbouillé, M., Augustyniak, K., Gilles, A.-M. & Wandersman, C.

Staphylococcus aureus FepA and FepB proteins drive heme iron utilization in *Escherichia coli*. *PLoS One* **8**, e56529 (2013).

84. Biswas, L. *et al.* Role of the twin-arginine translocation pathway in *Staphylococcus*. *J. Bacteriol.* **191**, 5921–9 (2009).
85. Cotton, J. L., Tao, J. & Balibar, C. J. Identification and characterization of the *Staphylococcus aureus* gene cluster coding for staphyloferrin A. *Biochemistry* **48**, 1025–35 (2009).
86. Cheung, J., Beasley, F. C., Liu, S., Lajoie, G. A. & Heinrichs, D. E. Molecular characterization of staphyloferrin B biosynthesis in *Staphylococcus aureus*. *Mol. Microbiol.* **74**, 594–608 (2009).
87. Dale, S. E., Doherty-Kirby, A., Lajoie, G. & Heinrichs, D. E. Role of siderophore biosynthesis in virulence of *Staphylococcus aureus*: identification and characterization of genes involved in production of a siderophore. *Infect. Immun.* **72**, 29–37 (2004).
88. Sebulsky, M. T. & Heinrichs, D. E. Identification and characterization of *fhuD1* and *fhuD2*, two genes involved in iron-hydroxamate uptake in *Staphylococcus aureus*. *J. Bacteriol.* **183**, 4994–5000 (2001).
89. Beasley, F. C., Marolda, C. L., Cheung, J., Buac, S. & Heinrichs, D. E. *Staphylococcus aureus* transporters Hts, Sir, and Sst capture iron liberated from human transferrin by Staphyloferrin A, Staphyloferrin B, and catecholamine stress hormones, respectively, and contribute to virulence. *Infect. Immun.* **79**, 2345–55 (2011).
90. Sheldon, J. R. & Heinrichs, D. E. The iron-regulated staphylococcal lipoproteins. *Front. Cell. Infect. Microbiol.* **2**, 41 (2012).
91. Hannauer, M., Sheldon, J. R. & Heinrichs, D. E. Involvement of major facilitator superfamily proteins SfaA and SbnD in staphyloferrin secretion in *Staphylococcus aureus*. *FEBS Lett.* **589**, 730–7 (2015).
92. Sheldon, J. R., Marolda, C. L. & Heinrichs, D. E. TCA cycle activity in *Staphylococcus aureus* is essential for iron-regulated synthesis of staphyloferrin A, but not staphyloferrin B: the benefit of a second citrate synthase. *Mol. Microbiol.* **92**, 824–39 (2014).
93. Konetschny-Rapp, S., Jung, G., Meiwes, J. & Zähner, H. Staphyloferrin A: a structurally new siderophore from staphylococci. *Eur. J. Biochem.* **191**, 65–74 (1990).
94. Kobylarz, M. J. *et al.* Synthesis of L-2,3-diaminopropionic acid, a siderophore and

antibiotic precursor. *Chem. Biol.* **21**, 379–88 (2014).

95. Cheung, J., Murphy, M. E. P. & Heinrichs, D. E. Discovery of an iron-regulated citrate synthase in *Staphylococcus aureus*. *Chem. Biol.* **19**, 1568–78 (2012).
96. Dale, S. E., Sebulsky, M. T. & Heinrichs, D. E. Involvement of SirABC in iron-siderophore import in *Staphylococcus aureus*. *J. Bacteriol.* **186**, 8356–62 (2004).
97. Grigg, J. C., Cheung, J., Heinrichs, D. E. & Murphy, M. E. P. Specificity of Staphyloferrin B recognition by the SirA receptor from *Staphylococcus aureus*. *J. Biol. Chem.* **285**, 34579–88 (2010).
98. Speziali, C. D., Dale, S. E., Henderson, J. A., Vinés, E. D. & Heinrichs, D. E. Requirement of *Staphylococcus aureus* ATP-binding cassette-ATPase FhuC for iron-restricted growth and evidence that it functions with more than one iron transporter. *J. Bacteriol.* **188**, 2048–55 (2006).
99. Arifin, A. J., Hannauer, M., Welch, I. & Heinrichs, D. E. Deferoxamine mesylate enhances virulence of community-associated methicillin resistant *Staphylococcus aureus*. *Microbes Infect.* **16**, 967–72 (2014).
100. Sandrini, S. M. *et al.* Elucidation of the mechanism by which catecholamine stress hormones liberate iron from the innate immune defense proteins transferrin and lactoferrin. *J. Bacteriol.* **192**, 587–94 (2010).
101. Morrissey, J. A., Cockayne, A., Hill, P. J. & Williams, P. Molecular cloning and analysis of a putative siderophore ABC transporter from *Staphylococcus aureus*. *Infect. Immun.* **68**, 6281–8 (2000).
102. Proctor, R. A. *et al. Staphylococcus aureus* Small Colony Variants (SCVs): a road map for the metabolic pathways involved in persistent infections. *Front. Cell. Infect. Microbiol.* **4**, 99 (2014).
103. Proctor, R. A., van Langevelde, P., Kristjansson, M., Maslow, J. N. & Arbeit, R. D. Persistent and relapsing infections associated with small-colony variants of *Staphylococcus aureus*. *Clin. Infect. Dis.* **20**, 95–102 (1995).
104. Proctor, R. A. *et al.* Small colony variants: a pathogenic form of bacteria that facilitates persistent and recurrent infections. *Nat. Rev. Microbiol.* **4**, 295–305 (2006).
105. Roggenkamp, A. *et al.* Chronic prosthetic hip infection caused by a small-colony variant of *Escherichia coli*. *J. Clin. Microbiol.* **36**, 2530–4 (1998).

106. Bryan, L. E. & Kwan, S. Aminoglycoside-resistant mutants of *Pseudomonas aeruginosa* deficient in cytochrome d, nitrite reductase, and aerobic transport. *Antimicrob. Agents Chemother.* **19**, 958–64 (1981).
107. Kahl, B. C., Becker, K. & Löffler, B. Clinical significance and pathogenesis of staphylococcal small colony variants in persistent infections. *Clin. Microbiol. Rev.* **29**, 401–27 (2016).
108. Wolter, D. J. *et al. Staphylococcus aureus* small-colony variants are independently associated with worse lung disease in children with cystic fibrosis. *Clin. Infect. Dis.* **57**, 384–91 (2013).
109. Musher, D. M., Baughn, R. E., Templeton, G. B. & Minuth, J. N. Emergence of variant forms of *Staphylococcus aureus* after exposure to gentamicin and infectivity of the variants in experimental animals. *J. Infect. Dis.* **136**, 360–9 (1977).
110. Massey, R. C., Buckling, A. & Peacock, S. J. Phenotypic switching of antibiotic resistance circumvents permanent costs in *Staphylococcus aureus*. *Curr. Biol.* **11**, 1810–1814 (2001).
111. Leimer, N. *et al.* Nonstable *Staphylococcus aureus* small-colony variants are induced by low pH and sensitized to antimicrobial therapy by phagolysosomal alkalinization. *J. Infect. Dis.* **213**, 305–13 (2016).
112. Edwards, A. M. Phenotype switching is a natural consequence of *Staphylococcus aureus* replication. *J. Bacteriol.* **194**, 5404–12 (2012).
113. von Eiff, C. *et al.* A site-directed *Staphylococcus aureus hemB* mutant is a small-colony variant which persists intracellularly. *J. Bacteriol.* **179**, 4706–12 (1997).
114. Bates, D. M. *et al. Staphylococcus aureus menD* and *hemB* mutants are as infective as the parent strains, but the menadione biosynthetic mutant persists within the kidney. *J. Infect. Dis.* **187**, 1654–61 (2003).
115. Dean, M. A., Olsen, R. J., Long, S. W., Rosato, A. E. & Musser, J. M. Identification of point mutations in clinical *Staphylococcus aureus* strains that produce small-colony variants auxotrophic for menadione. *Infect. Immun.* **82**, 1600–5 (2014).
116. Lannergård, J. *et al.* Identification of the genetic basis for clinical menadione-auxotrophic small-colony variant isolates of *Staphylococcus aureus*. *Antimicrob. Agents Chemother.* **52**, 4017–22 (2008).
117. Schaaff, F., Bierbaum, G., Baumert, N., Bartmann, P. & Sahl, H. Mutations are involved in

emergence of aminoglycoside-induced small colony variants of *Staphylococcus aureus*. *Int. J. Med. Microbiol.* **293**, 427–35 (2003).

118. Johansson, P. & Hederstedt, L. Organization of genes for tetrapyrrole biosynthesis in Gram-positive bacteria. *Microbiology* **145 (Pt 3**, 529–538 (1999).
119. Hammer, N. D. *et al.* Inter- and intraspecies metabolite exchange promotes virulence of antibiotic-resistant *Staphylococcus aureus*. *Cell Host Microbe* **16**, 531–7 (2014).
120. Seggewiss, J. *et al.* Reporter metabolite analysis of transcriptional profiles of a *Staphylococcus aureus* strain with normal phenotype and its isogenic *hemB* mutant displaying the small-colony-variant phenotype. *J. Bacteriol.* **188**, 7765–77 (2006).
121. Kriegeskorte, A. *et al.* Small colony variants of *Staphylococcus aureus* reveal distinct protein profiles. *Proteomics* **11**, 2476–90 (2011).
122. von Eiff, C. *et al.* Phenotype microarray profiling of *Staphylococcus aureus menD* and *hemB* mutants with the small-colony-variant phenotype. *J. Bacteriol.* **188**, 687–93 (2006).
123. Kohler, C. *et al.* Physiological characterization of a heme-deficient mutant of *Staphylococcus aureus* by a proteomic approach. *J. Bacteriol.* **185**, 6928–37 (2003).
124. Vaudaux, P. *et al.* Increased expression of clumping factor and fibronectin-binding proteins by *hemB* mutants of *Staphylococcus aureus* expressing small colony variant phenotypes. *Infect. Immun.* **70**, 5428–37 (2002).
125. Tuchscherr, L. *et al. Staphylococcus aureus* small-colony variants are adapted phenotypes for intracellular persistence. *J. Infect. Dis.* **202**, 1031–40 (2010).
126. Mitchell, G. *et al.* SigB is a dominant regulator of virulence in *Staphylococcus aureus* small-colony variants. *PLoS One* **8**, e65018 (2013).
127. Novick, R. P. & Geisinger, E. Quorum sensing in staphylococci. *Annu. Rev. Genet.* **42**, 541–564 (2008).
128. Kriegeskorte, A. *et al. Staphylococcus aureus* small colony variants show common metabolic features in central metabolism irrespective of the underlying auxotrophism. *Front. Cell. Infect. Microbiol.* **4**, 141 (2014).
129. Sebulsky, M. T., Speziali, C. D., Shilton, B. H., Edgell, D. R. & Heinrichs, D. E. FhuD1, a ferric hydroxamate-binding lipoprotein in *Staphylococcus aureus*: a case of gene duplication and lateral transfer. *J. Biol. Chem.* **279**, 53152–9 (2004).
130. Hannauer, M., Arifin, A. J. & Heinrichs, D. E. Involvement of reductases IruO and NtrA in

iron acquisition by *Staphylococcus aureus*. *Mol. Microbiol.* **96**, 1192–210 (2015).

131. Bateman, B. T., Donegan, N. P., Jarry, T. M., Palma, M. & Cheung, a L. Evaluation of a tetracycline-inducible promoter in *Staphylococcus aureus in vitro* and *in vivo* and its application in demonstrating the role of *sigB* in microcolony formation. *Infect. Immun.* **69**, 7851–7 (2001).
132. Diep, B. A. *et al.* Complete genome sequence of USA300, an epidemic clone of community-acquired meticillin-resistant *Staphylococcus aureus*. *Lancet* **367**, 731–9 (2006).
133. Bae, T. & Schneewind, O. Allelic replacement in *Staphylococcus aureus* with inducible counter-selection. *Plasmid* **55**, 58–63 (2006).
134. Laakso, H. A., Marolda, C. L., Pinter, T. B., Stillman, M. J. & Heinrichs, D. E. A heme-responsive regulator controls synthesis of staphyloferrin B in *Staphylococcus aureus*. *J. Biol. Chem.* **291**, 29–40 (2016).
135. Drechsel, H. *et al.* Purification and chemical characterization of staphyloferrin B, a hydrophilic siderophore from staphylococci. *Biometals* **6**, 185–92 (1993).
136. Lewis, L. A., Lewis, D., Persaud, V., Gopaul, S. & Turner, B. Transposition of IS2 into the *hemB* gene of *Escherichia coli* K-12. *J. Bacteriol.* **176**, 2114–20 (1994).
137. Echelard, Y., Dymetryszyn, J., Drolet, M. & Sasarman, A. Nucleotide sequence of the *hemB* gene of *Escherichia coli* K12. *Mol. Gen. Genet.* **214**, 503–8 (1988).
138. Malone, J. G. Role of small colony variants in persistence of *Pseudomonas aeruginosa* infections in cystic fibrosis lungs. *Infect. Drug Resist.* **8**, 237–47 (2015).
139. Irvine, S. *et al.* Genomic and transcriptomic characterization of *Pseudomonas aeruginosa* small colony variants derived from a chronic infection model. *Microb. genomics* **5**, 1–11 (2019).
140. Frankenberg, N., Kittel, T., Hungerer, C., Römling, U. & Jahn, D. Cloning, mapping and functional characterization of the *hemB* gene of *Pseudomonas aeruginosa*, which encodes a magnesium-dependent 5-aminolevulinic acid dehydratase. *Mol. Gen. Genet.* **257**, 485–9 (1998).
141. Gstraunthaler, G., Lindl, T. & van der Valk, J. A plea to reduce or replace fetal bovine serum in cell culture media. *Cytotechnology* **65**, 791–3 (2013).
142. Garcia, L. G. *et al.* Pharmacodynamic evaluation of the activity of antibiotics against hemin- and menadione-dependent small-colony variants of *Staphylococcus aureus* in models of

extracellular (broth) and intracellular (THP-1 monocytes) infections. *Antimicrob. Agents Chemother.* **56**, 3700–11 (2012).

143. Wong Fok Lung, T. *et al. Staphylococcus aureus* small colony variants impair host immunity by activating host cell glycolysis and inducing necroptosis. *Nat. Microbiol.* **5**, 141–153 (2020).
144. Flannagan, R. S. & Heinrichs, D. E. Macrophage-driven nutrient delivery to phagosomal *Staphylococcus aureus* supports bacterial growth. *EMBO Rep.* e50348 (2020). doi:10.15252/embr.202050348
145. Noiva, R., Pete, M. J. & Babin, D. R. Bovine serum hemopexin: properties of the protein from a single animal. *Comp. Biochem. Physiol. B.* **88**, 341–7 (1987).
146. Becker, K., Heilmann, C. & Peters, G. Coagulase-negative staphylococci. *Clin. Microbiol. Rev.* **27**, 870–926 (2014).
147. Perry, W. J. *et al. Staphylococcus aureus* exhibits heterogeneous siderophore production within the vertebrate host. *Proc. Natl. Acad. Sci. U. S. A.* **116**, 21980–21982 (2019).
148. Jonsson, I.-M. *et al.* Virulence of a *hemB* mutant displaying the phenotype of a *Staphylococcus aureus* small colony variant in a murine model of septic arthritis. *Microb. Pathog.* **34**, 73–9 (2003).
149. Brouillette, E., Martinez, A., Boyll, B. J., Allen, N. E. & Malouin, F. Persistence of a *Staphylococcus aureus* small-colony variant under antibiotic pressure *in vivo*. *FEMS Immunol. Med. Microbiol.* **41**, 35–41 (2004).
150. Pollitt, E. J. G., Szkuta, P. T., Burns, N. & Foster, S. J. *Staphylococcus aureus* infection dynamics. *PLoS Pathog.* **14**, e1007112 (2018).
151. Spaans, S. K., Weusthuis, R. A., van der Oost, J. & Kengen, S. W. M. NADPH-generating systems in bacteria and archaea. *Front. Microbiol.* **6**, 742 (2015).
152. Kobylarz, M. J., Heieis, G. A., Loutet, S. A. & Murphy, M. E. P. Iron uptake oxidoreductase (IruO) uses a flavin adenine dinucleotide semiquinone intermediate for iron-siderophore reduction. *ACS Chem. Biol.* **12**, 1778–1786 (2017).
153. Tavares, A. F. N., Nobre, L. S., Melo, A. M. P. & Saraiva, L. M. A novel nitroreductase of *Staphylococcus aureus* with S-nitrosoglutathione reductase activity. *J. Bacteriol.* **191**, 3403–6 (2009).
154. Brickman, T. J. & McIntosh, M. A. Overexpression and purification of ferric enterobactin

esterase from *Escherichia coli*. Demonstration of enzymatic hydrolysis of enterobactin and its iron complex. *J. Biol. Chem.* **267**, 12350–5 (1992).

155. Miethke, M. *et al.* Ferri-bacillibactin uptake and hydrolysis in *Bacillus subtilis*. *Mol. Microbiol.* **61**, 1413–27 (2006).
156. Kohler, C. *et al.* A defect in menadione biosynthesis induces global changes in gene expression in *Staphylococcus aureus*. *J. Bacteriol.* **190**, 6351–64 (2008).
157. Baddour, L. M., Simpson, W. A., Weems, J. J., Hill, M. M. & Christensen, G. D. Phenotypic selection of small-colony variant forms of *Staphylococcus epidermidis* in the rat model of endocarditis. *J. Infect. Dis.* **157**, 757–63 (1988).
158. Tande, A. J. *et al.* Clinical characteristics and outcomes of prosthetic joint infection caused by small colony variant staphylococci. *MBio* **5**, 1–9 (2014).

Curriculum Vitae

Name Izabela Z. Batko

Education

- M.Sc. in Microbiology and Immunology, University of Western Ontario, London, ON. 2018-2020.
- B.M.Sc. Honours Specialization in Microbiology and Immunology, University of Western Ontario, London, ON. 2014-2018.

Honours and Awards

- Western Graduate Research Scholarship. 2018-2020.
- Dr. Frederick W. Luney Graduate Travel Award in Microbiology and Immunology. 2019.
- Dr. Frederick W. Luney Graduate Entrance Scholarship in Microbiology and Immunology, 2018.
- Dean's Honour Role, University of Western Ontario, London, ON. 2014-2018.
- Western Scholarship of Excellence. 2014.

Related Volunteer and Work Experience

- Member of Infection and Immunity Research Forum (IIRF) planning committee, University of Western Ontario, London, ON. 2018-2020.
- Teaching assistant in the undergraduate course MicroImm 3100A: Microbiology, University of Western Ontario, London, ON. 2018-2020.

Poster Presentations

- I. Z. Batko, R. S. Flannagan, D. E. Heinrichs. Examination of iron acquisition strategies employed by *Staphylococcus aureus* small colony variants. Infection and Immunity Research Forum, University of Western Ontario, London, ON. November 2019.
- I. Z. Batko, R. S. Flannagan, D. E. Heinrichs. Examination of iron acquisition strategies employed by *Staphylococcus aureus* small colony variants. 69th Annual Conference of the Canadian Society of Microbiologists, Sherbrooke, Quebec, Canada. June 2019.